Advanced Ceramics Progress: Vol. 7, No. 3, (Summer 2021) 29-48

Materials and Energy Research Center
MERC

Contents lists available at ACERP

Advanced Ceramics Progress

Journal Homepage: www.acerp.ir

**Original Research Article**

# Chloride Ingress into High-Performance Concrete Containing Graphene Oxide Nanoplatelets and Ground Granulated Blast Furnace Slag under Different Conditions of Water Pressure and Temperature

D. Rezakhani [a], A. H. Jafari [b,*], M. A. Hajabbasi [c]

[a] *PhD Student, Department of Materials Science and Engineering, Faculty of Engineering, Shahid Bahonar University of Kerman, Kerman, Kerman, Iran*
[b] *Associate Professor, Department of Materials Science and Engineering, Faculty of Engineering, Shahid Bahonar University of Kerman, Kerman, Kerman, Iran*
[c] *Assistant Professor, Department of Materials Science and Engineering, Faculty of Engineering, Shahid Bahonar University of Kerman, Kerman, Kerman, Iran*

* Corresponding Author Email: jafham2020@gmail.com (A. H. Jafari)

URL: https://www.acerp.ir/article_139023.html

*ARTICLE INFO*

*Article History:*

Received 10 September 2021
Received in revised form 15 October 2021
Accepted 19 October 2021

*Keywords*:

Concrete
Diffusion
Chloride Ion
Graphene Oxide Nanoplatelet
Ground Granulated Blast Furnace Slag

*ABSTRACT*

In this study, concrete samples were prepared by adding 0.1 wt. % Graphene Oxide (GO) and 50 wt. % Ground Granulated Blast Furnace Slag (GGBFS). Tests on the mechanical and chloride permeation properties were also conducted. Concrete samples were exposed to pressurized 3.5 % NaCl aqueous solution under a certain time and temperature condition. The water pressures were 0.1, 0.3, and 0.7 MPa, respectively. The chloride concentration profiles under different conditions were measured. The results indicated that addition of 0.1 wt. % GO and 50 wt. % GGBFS would increase the compressive strength of the concrete sample up to 19.9 % during 28 days and 17.6 % during 90 days compared to ordinary concrete sample. Concrete with a combination of 0.1 wt. % graphene oxide and 50 wt. % granular slag witnessed an increase in its flexural strength up to 15 % during 28 days and 13.6 % during 90 days. Compared to the ordinary concrete, 90-day cured concrete containing GGBFS and GO undergone high reduction in Rapid Chloride Permeability (RCP) from 4012 C to 1200 C. Chloride ion content was substantially enhanced upon increasing water pressure and exposure time. In this study, convection-diffusion coupling was the main mechanism of the chloride ion transfer in the concrete. The mix with 0.1 wt. % GO and 50 wt. % GGBFS exhibited acceptable performance in terms of chloride penetration in the concrete. Compared to ordinary concrete, this admixure reduced the chloride penetration by 17.6 % in 90 days. Chloride ion penetration was curtailed while adding GO and GGBFS to the ordinary concrete. The effects of pozolanic reaction in the concrete leading to the filling of the pores were significant factors in the proposed curtailment mechanism.

https://doi.org/10.30501/ACP.2021.304143.1072

## 1. INTRODUCTION

Hydrostatic water pressure can lead to rapid chloride diffusion into the concrete, establishment of concentration gradients in different directions, and its spread through the mass of marine structure [1-3]. The surface of the concrete exposed to the environment may experience dry and wet cycles, and in the presence of

Please cite this article as: Rezakhani, D., Jafari, A. H., Hajabbasi, M. A., "Chloride Ingress into High-Performance Concrete Containing Graphene Oxide Nanoplatelets and Ground Granulated Blast Furnace Slag under Different Conditions of Water Pressure and Temperature", ***Advanced Ceramics Progress***, Vol. 7, No. 3, (2021), 29-48. https://doi.org/10.30501/ACP.2021.304143.1072

dissolved chlorine ion, it will diffuse into the concrete [4]. Even if the concrete is dense and thick, chloride ions will eventually reach the interface of any rebar inside the structure. The rate of chlorine ion penetration into the concrete depends on its matrix structure, which itself is controlled by the quality of used materials and concrete preparation process [1]. Parameters such as the water-to-cement ratio, gravel and sand, especially the additives and cement replacement materials, and degree of hydration process can significantly determine the final structure of the concrete. In the marine environments, the immersion depth and temperature also critically affect the ingression [4]. Many parameters affect the durability of the reinforced concrete structures in coastal and offshore marine environments with chloride-induced corrosion of rebar as a key problem [5,6]. Generally, concretes form a passive layer on the steel rebar which protects it from corrosion; however, chloride ions from marine environment diffused into the concrete will damage this layer that initiates corrosion [7-9]. Efforts have been made to minimize chlorine penetration into the concrete, including replacing cement with admixtures such as GGBFS and additives like Carbon nanotubes (CNTs), Carbon nanofibers (CNFs), Nano-$SiO_2$ and nano-$TiO_2$ particles, Graphene, and Graphene Oxide (GO) nanoplatelets [10-16].

Ying et al. showed that addition of Nano-$SiO_2$ and nano-$TiO_2$ particles refined the pore structure of Recycled Aggregate Concrete (RAC) and enhanced its resistance to chloride diffusivity of RAC. They also found that Nano-$TiO_2$ slightly outperformed Nano-$SiO_2$ in terms of refining RAC [16]. In comparison with Natural Aggregate Concrete (NAC), RAC is more porous because of the old adhered cement and its total porosity, and the average pore diameter increased with an increase in the Recycled Coarse Aggregate (RCA) content [16]. Ying et al. examined the effects of RCA distribution on chloride diffusion with different RCA replacement ratios. The results indicated that chloride diffusivities of the RAC would generally increase with an increase in the RCA replacement ratios [17].

Ground Granulated Blast Furnace Slag (GGBFS) is a green mineral admixture that improves both mechanical and durability properties. Replacement of slag with Portland cement is beneficial since it reduces cement consumption in the concrete and $CO_2$ emissions in the global cement industry[18]. Further, addition of slag modifies the hydration process and physico-chemical properties (such as porosity and transport properties) of cementitious materials [19]. Teng et al. showed that concrete with GGBFS was characterized by higher strength, lower permeability, and improved durability [20]. Sideris investigated the mechanical characteristics and durability of Self-Compacting Concrete (SCC) produced from ladle furnace slag. According to the findings, slag enhanced the durability characteristics of the concrete, thus leading to environmentally-friendly concrete mixtures with lower cost [21]. Chen et al. evaluated the effect of curing conditions on the strength, porosity, and chloride ingress characteristics of concretes made of High Slag Blast Furnace Cement (HBFC) and Ordinary Portland Cement (OPC). The results indicated that the HBFC concretes exhibited higher resistance to chlorides ion penetration than the OPC concretes [22]. Boucetta et al. employed Glass Powder (GP) obtained from the recovery of glass bottles and Granulated Slag (GS) of blast furnaces as admixtures in the concrete. Accordng to the conducted tests, incorporation of GP and GS would improve the mechanical strength of concretes and reduce the capillary water absorption and chloride ion diffusion [23]. Özbay et al. reported that in concretes, where 40, 60, and 80 wt. % slag was replaced by cement, exhibited much higher strength with 60 wt. % slag showing the maximum tensile and flexural strength [15]. Fan et. al used the slag/fly ash as the binding material. Their results revealed that the interfacial bond strength of the concrete increased significantly when the slag content was 50 wt. %, which was 62 % higher than that of OPC. Compared to OPC, this concrete exhibited the best chloride penetration resistance in the case of 50 wt. % slag content. In addition, some reactions occured between the alkali activated slag and cement, hydrated calcium silicate (C-S-H), and hydrated calcium aluminate (C-A-H) gels [24]. Chen et al. showed that the apparent chloride diffusion coefficient decreased with an increase in the exposure time, followed by an exponential relationship. In their study, slag had a positive effect on the concrete resistance to chloride penetration [18]. According to the conducted studies, GGBFS-added concretes are slow at gaining the maximum strength, but this can be counteracted by temperature during curing. [25-29]. Shi et al. evaluated the effect of GGBS addition on the chloride penetration into the concrete and found that 50 wt. % or more GGBFS could reduce permeability [25]. Ramezanianpour studied the penetration of chloride ion in concrete samples with 50 wt. % slag during for 1, 28, and 180 days. The results showed 26.64 %, 74.52 %, and 82.58 % reduction in the chloride ion diffusion in 1, 28, and 180 days, respectively [30]. Bagheri et al. observed that chlorine ion permeability decreased in concrete samples containing 50 % slag with a curing time of 28, 90, and 180 days [31]. Jau and Tsai also reported a decrease in the concentration of chloride ions in concrete samples by replacing 50 % slag with cement compared to ordinary concrete samples [32]. Haj Sadok et al. studied chloride permeation in concrete samples containing 50 % slag. The results showed that less chloride ion penetration occurred in concrete samples containing 50 % slag during 270 days [33]. Sengul and Tasdemir observed lower penetration of chloride ions in concrete samples containing slag as a cement substitute [34]. Kayali et al. observed 35 % and 24 % reduction in the charge passed (Coulombs) of concrete specimens at the age of 350 days including 50 % and 70 % slag, respectively [35]. Yeau

and Kim showed that the chloride ion diffusion coefficient of concrete samples decreased after 28 days with partial replacement of cement with 55 % slag compared to ordinary concrete [36]. Through accelerated tests, Cheng et al. observed a significant decrease in the chlorine ion permeability among concrete samples containing 60 % slag [37]. Gupta employed a type of cement with 60 % slag to reduce the water penetration depth among 28- and 90-day concrete samples [38]. Dhir et al. observed lower chloride penetration into concretes containing 50 % and 66.7 % slag on 28 days of age. In this study, upon increasing the amount of slag , the permeability of chlorine ion would decrease [39]. Berndt observed lower chloride permeability among concrete samples during a year by replacing the cement with 50 % and 70 % slag [40]. Thomas et al. showed that concretes with 45 % and 65% slag as a cement substituted by a lower water/binder ratio reduced the chloride penetration after 25 years of tidal exposure. The chloride permeability further decreased by increasing slag content [41]. Mo et al. found 23.72 % reduction in the 28-day compressive strength of concrete specimens by partial replacement of cement with 60 % slag [42]. Gsoglu et al. showed 10.73 % reduction in 90-day compressive strength of concrete samples with 60 % slag as a cement substitute [43]. Aly and Sanjayan observed 82.89 and 54.54 reduction in the compressive strength of one- and seven-day concrete samples by partial replacement of cement with 65 % slag [44]. Elahi et al. found lower chloride diffusion coefficient of concrete samples by partial replacement of cement with 50 % and 70 % slag [45]. McNally and Sheils showed that 50-70 % slag in the concrete contributed to the reduction in the chloride diffusion in the service life of 50 and 100 years [46]. Aprianti et al. observed less porosity in the concrete containing 50 % slag than that in the ordinary concrete [47]. Nazari and Riahi studied several researches on microstructural, thermal, physical and mechanical behavior of the self compacting concrete [48-53].They reported that use of 45 % and 60 % slag in concrete as a substitute for cement reduced the seven-day compressive strength and increased it at 28 and 90 days of age [50]. Johari et al. showed that as a result of using 60 % slag as a cement substitute the porosity of mortar samples was reduced at the age 28 days [54].

Currently, several studies have been conducted on the effect of GO on the microstructure and mechanical properties of cement-based composites. According to a number of these studies, changes in the mechanical properties were mainly caused by changes at the micro level. Lyu et al. believed that a combination of the right amount of GO could significantly improve the microstructure of the mortar mainly due to its sigjnificant role in the formation of cement hydration products [55]. The results obtained by Mohammad et al. revealed that composition of GO could not only improve the compaction and pore structure of cement mortar but also prevent the spread of fine cracks in cement mortar [56]. Many other studies have shown that GO could create a denser microstructure of cement-based materials and reduce the total pore volume of the cementitious composite [57-62]. Wang et al. showed that the main reasons why GO could improve the mechanical strength of cement-based materials were to promote secondary hydration, reduce pore volume, and refine CH crystals [63]. Yang et al. confirmed that GO had no effect on the structure of C-S-H, and that the improvement of its mechanical properties resulted from the acceleration of hydration [64]. According to their findings, followed by addition of 0.2 wt. % GO [64], the compressive strength of cement-based composite increased up to 42.3 % and 35.7 % in three and seven days, respectively. Liu et al. evaluated the correlation between the damage development in concrete and resistivity reaction of cementitious composites infilled with Graphene Nano-Platelets (GNPs). They also showed that the piezoresistivity of smart concrete containing GNPs could be a promising tool for detecting damages in detail [65]. Xu et al. reported that GNPs additive could reduce the diffusion coefficient of chloride ion into the cement matrix [66]. Somasri and Kumar showed that GNPs were incorporated into the concrete to improve the performance characteristics [67]. Lv et al. reported 78.6 %, 6.6 %, and 39.9 % increase in the tensile strength, flexural strength, and compressive strength, respectively, as a result of adding just 0.03 wt. % Graphene Oxide [68]. Gong et al. reported that adding 0.63 wt. % GNPs would result in a 40 % increase in both compressive strength and tensile strength of the concrete due to the reduction in the pore size in the cement matrix as well as enhanced cement hydration rate [69]. Of note, GNPs surface is suitable for C-S-H nucleation, thus enhancing the hydration process [70]. Jiang et al. showed that adding GO would decrease the porosity and proportion of large capillary pores curtailing the diffusion of chloride [71]. In addition, temperature could significantly affect diffusion with an adequate temperature gradient providing the driving force for chloride ion diffusion [72-74]. Isteita et al. found that coupled temperature and chloride concentration gradients appreciably increased the diffusion rate of chloride [74]. On the contraty, Yuan et al. and Nguyen et al. showed that higher temperature would result in enhanced chloride diffusion and greater permeation depth [75,76]. Al-Khaja studied the durability of high-strength and ordinary concrete exposed to 5 % NaCl environments at temperatures of 20 and 45 °C and reported a significant increase in the chloride ingress with temperature [77]. Other researchers have proposed some models and took into account both temperature and pressure in their modeling for silica fume, slag, and fly-ash containing concretes [78-85].

Nowadays, under different environmental conditions, structures do not function as expected. Damages in the form of structural cracks caused by stress as well as

scaling and shrinkage caused by loss of fine aggregates and high wear, leakage, etc. lead to the failure of concrete structures. In addition, use of ordinary concrete leads to premature destruction of structures. Therefore, use of high-strength concrete containing GGBFS and GO as a building material in marine structures can be useful. Using such high-performance concretes can reduce the cost of materials by reducing the thickness of the structure, increasing the mechanical, physical and corrosion properties, and saving the required materials. As predicted, addition of GGBFS and GO enhanced both compressive and flexural strength as well as resistance to chloride permeation into the concrete. Moreover, use of GGBFS and GO in the concrete is progressing due to its exceptional properties. Further, incorporation of GGBFS and GO would increases the compressive and tensile strength of the concrete and its resistance to chloride permeation into the concrete, mainly due to reduction in pore size in the cement matrix as well as enhanced cement hydration rate. GO has become popular and widely used in different fields around the world since it is cheaper than multi-walled CNTs, single-walled CNTs and CNFs (which are 250, 1280, and 218 times more expensive than GO per 100 g, respectively) [86].

Therefore, the mix of GGBFS and GO is the best candidate for this research. No study has been reported on GO and GGBFS inclusion in concrete composites with regards to chloride permeation to get a clear picture of whether or not this investigation will be helpful for practical application in construction industry. To this end, this study was carried out to develop a nano-reinforced concrete composite with addition of GO and GGBFS. The present study put the main focus on the application of GO-GGBFS as a nano-filler in developing a concrete for industrial applications in marine environment. In this paper, the chloride ion penetration into the ordinary concrete and that containing GO and GGBFS under different conditions was measured, taking into account the temperature, pressure, and time.

## 2. MATERIALS AND METHODS

The present study employed concrete mixes with the chemical composition and mechanical properties according to ASTM C109, ASTM C136, and ASTM C117 standards made from type II Portland cements to form samples. Samples were made according to ASTM C192M-16. The samples were kept in the mold in the laboratory for 24 hours and placed in a bath containing lime for 90 days at 25 °C and a relative humidity of 95 %. Both ordinary concrete and that containing 50 wt. % GGBFS and 0.1 wt. % GO were employed in this study. The mix was selected due to the good behavior of concrete with 50 wt. % slag and that with 0.1 wt. % graphene oxide independently in sources. In addition, 50 wt. % GGBFS substitution was as a cementing material in the concrete, and 0.1 wt. % GO as a additive. Table 1 shows the mixing ratio of the concretes. GGBFS with blaine fineness of 3500 $cm^2g^{-1}$ and $CaO/SiO_2$ ratio of 1.4 corresponding to ASTM E1621-13 was used as the cement replacement in samples containing graphene oxide. Infrared Fourier Transform Spectroscopy (FTIR) was empolyed to determine the amount and type of functional groups present in graphene oxide.

**Table 1.** Quantity of materials used in $m^3$ of concrete samples

| Materials | Mix | |
|---|---|---|
| | C1 (Ordinary Concrete) | C2 (Concrete Containing GGBFS and GO) |
| GGBFS (wt. %) | 0.00 | 50 |
| GO (wt. %) | 0.00 | 0.10 |
| GGBFS ($Kg/m^3$) | 0.00 | 212.5 |
| GO ($Kg/m^3$) | 0.0000 | 0.4250 |
| OPC ($kg/m^3$) | 425 | 212.5 |
| Water ($kg/m^3$) | 170 | 170 |
| FA ($kg/m^3$) | 1005.5 | 1005.5 |
| CA ($kg/m^3$) | 676.5 | 676.5 |
| SP($kg/m^3$) | 0.0425 | 0.0425 |

 OPC: Ordinary Portland Cement, GO: Graphene Oxide, GGBFS: Ground Granulated Blast Furnace Slag, FA: Fine Aggregate, CA: Coarse Aggregate, SP: (Carboxylate based) Super Plasticizer

ASTM C39M-18 and C78M-18 standard tests were carried out to examine the compression and flexural strength of concrete specimens. Chloride permeability resistance was evaluated per ASTM C1202 accelerated test [87]. The total coulombs of electricity thus passed, would be proportional to the electrical resistance of the specimen which, inversely relates to chloride ion penetrating the sample. So, the lower the electric current passed indicates higher resistance to chloride ingress. For determining the resistivity of concrete, Wenner test was applied with modifications based on AASTHO TP 95-11 standard [88,89]. Total porosity and pore size distribution were determined using mercury porosity (Mercury Intrusion Porosimetry-MIP) based on ASTM D4404 with a maximum pressure of 201 MPa. A contact angle of 140 degrees and pores between 10 and 1000 nm were selected. Further, permeation tests were performed on the specimens using the apparatus shown in Fig. 1. One side of the samples was exposed to 3.5 % NaCl solution from a especially constructed reservoir which enabled sealing the face in contact with solution which was then put in contact with water under pressure in the experiment duration. The existing Chinese standard JTJ270-98 was taken into consideration to build a penetration test set up [82]. Water pressures of 0.1, 0.3, and 0.7 MPa was exerted on the samples to determine the amount of chlorine ion in different immersion depths. Table 2 shows the factors and levels of permeation tests. After the time set for each test, the sample was removed from the

penetration test set-up, and its chloride content was determined based on ASTM C 1556 by drilling in six different depths with a 2.5 cm drill in the Z direction. Fig. 2 shows a schematic of concrete sampling on the drilling direction. Chloride content was measured through chemical analysis described in ASTM C1152 and ASTM C1218 and titration method according to ASTMC124. Titration with silver nitrate solution according to AASHTO T269 and ASTM C114 was taken into account to measure the complete concentration.

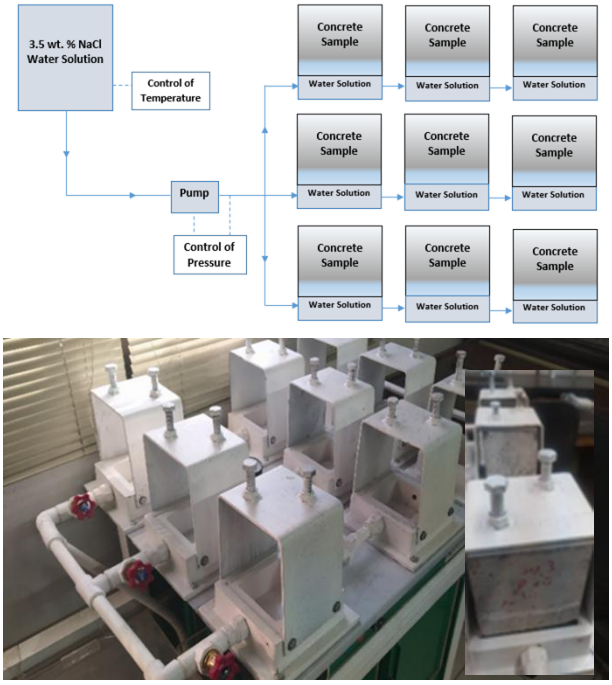


**Figure 1.** Permeability test set up to study chloride penetration under constant pressure and temperature

**Table 2.** Factors and levels of permeation tests

| Test Factor | Values | Level |
|---|---|---|
| Pressure | 0.1 MPa, 0.3 MPa, 0.7 MPa | 3 |
| Temperature | 25 °C, 35 °C, 55 °C | 3 |
| Pressuring Time | 24 h, 72 h, 144 h | 3 |
| Concrete Type | Ordinary Concrete, Concrete Containing GGBFS and GO | 2 |
| Test Samples | | 54 |

## 3. RESULTS AND DISCUSSION

Fig. 3 shows the FTIR spectroscopy results of the nanoparticles used in this study from Hummer method. As observed, Graphene oxide has different functional groups including hydroxyl, epoxy, carboxyl, phenol, ether, and aldehyde. The strong vibration band in the region of 3399.77 $cm^{-1}$ is attributed to the OH hydroxyl group resulting from moisture absorption. The tensile vibration bands in 1727.69 $cm^{-1}$ and 1620.71 $cm^{-1}$ are related to carbonyl bonds C=O and bond C=C, respectively. While the tensile vibration in 1364.36 $cm^{-1}$ band belong to C-OH bond, 1226.86 $cm^{-1}$ and 1064.76 $cm^{-1}$ belong to CO bond of epoxy group. The vibration band of 515.51 $cm^{-1}$ indicates CH bond. Peak intensities confirm the presence of these functional groups as the main groups in graphene nano-oxide after the oxidation process, which is consistent with the findings from the published literature [90]. X-Ray Diffraction (XRD) diagram of graphene nano-oxide used in this study is shown in Fig. 4. Based on the obtained diffraction spectrum, all peaks related to primary graphite are removed, and the only peak observed in the XRD spectrum is related to graphene oxide nano plates which is in agreement with the results from the literature [91,92].

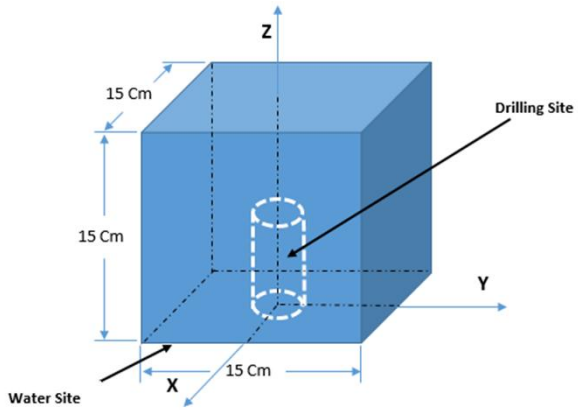


**Figure 2.** Schematic of concrete sample and sampling and powdering areas

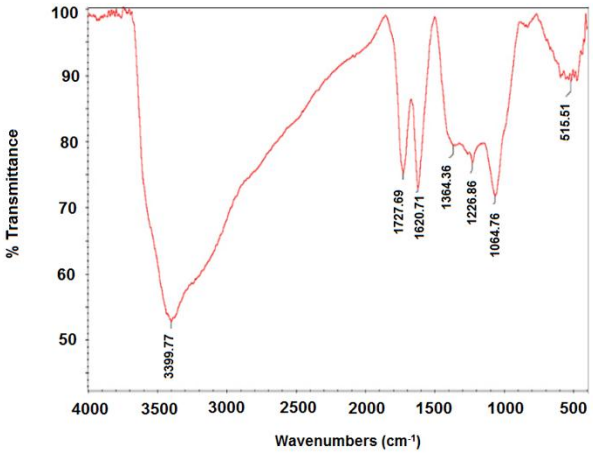


**Figure 3.** FTIR graph of GO produced by Hummer method

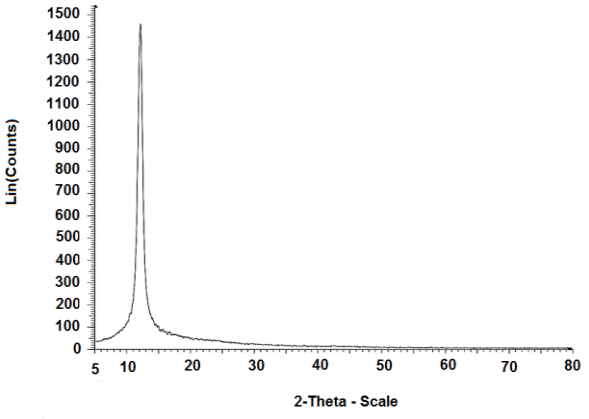


**Figure 4.** X-ray diffraction diagram (XRD) of GO

The singular peak shown at the scattering angle of 2θ = 12° corresponds to the (001) graphene oxide plate, and lack of any other peak is indicative of complete graphite oxidation and high purity of graphene oxide. The results confirmed that oxygenated functional groups were introduced between the primary graphite plates, thus weakening the interactions among them. This helps the graphene oxide sheets disperse more easily in aqueous solutions, hence prepeartion of a stable suspension. The plate spacing in the graphite structure is 2.9 to 3.6 Å and in the case of graphene oxide, it is about 7 Å, which is indicative of an increase in the distance between the primary graphite plates in the process of producing graphene oxide, thus confirming the entry of functional groups between the graphene oxide plates [91,93].

FE-SEM images from the powder sample in Fig. 5 show wrinkled thin layers, thus creating a porous lattice morphology that is somewhat a recognizable and distinctive feature of the material, as previously reported by other researchers [94-104]. According to this figure, the dimensions of the graphene oxide plates range from 2 to 15 µm, and the average thickness of the plates is about 7.7 nm. The results of XRD and XRF analysis of GGBFS used in this research are shown in Fig. 6 and Table 3, respectively. According to Table 3, the main constituents are CaO and $SiO_2$, followed by $Al_2O_3$ and MgO. The main peaks belong to $Ca_2MgSi_2O_7$, $Ca_2Al_2SiO_7$, and $Ca_2SiO_4$ (as shown in Fig. 6 as red, green, and blue lines) that are in accordance with the results from previous sources [105]. According to ASTM E1621, and results given in Table 3, the ratio of CaO to $SiO_2$ is calcuated as 1.4.

Fig. 7 presents the results of the mechanical and physical tests for samples of 28 and 90 curing days, showing marginal improved compressive strength, flexural strength, electrical resistivity, and electrical conductivity in the concrete containing GGBFS and GO at the curing time of 28 and 90 days.

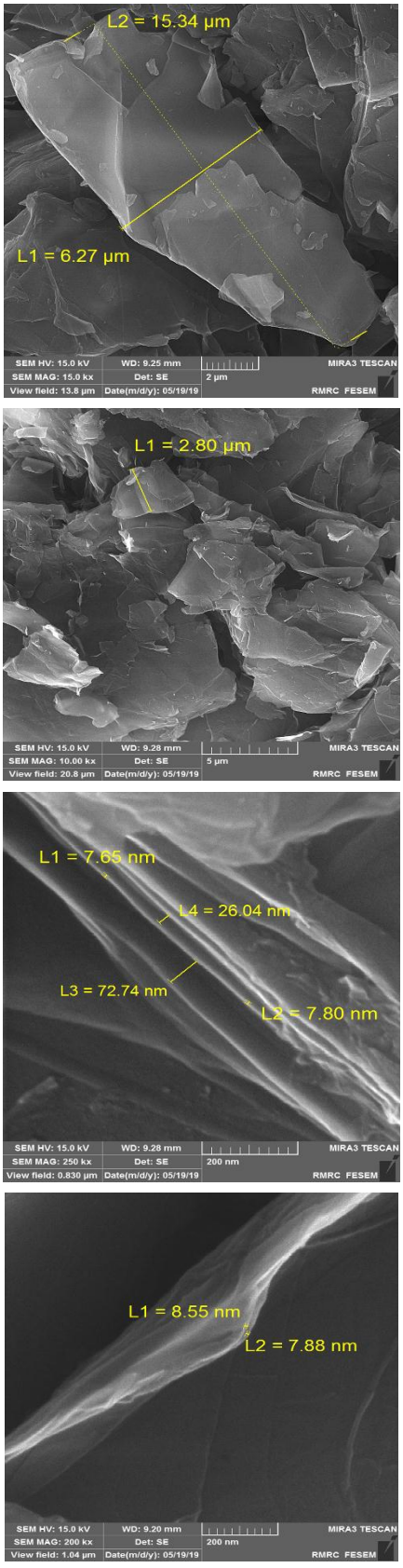


**Figure 5.** FE-SEM images of graphene oxide nano sheets

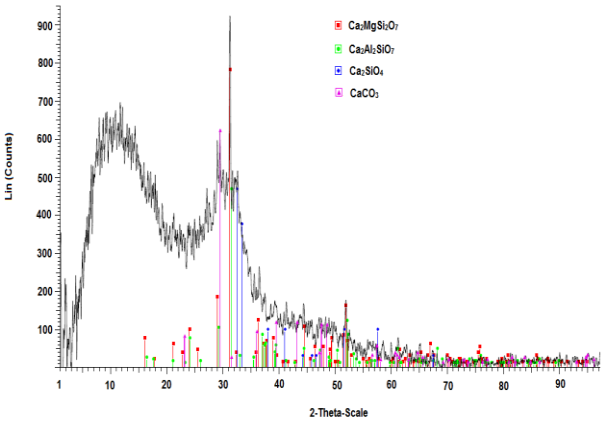


**Figure 6.** XRD analysis of granular slag

**Table 3.** XRF analysis of granular slag

| Constituent | % |
|---|---|
| $Na_2O$ | 0.55 |
| $P_2O_5$ | 0.06 |
| CaO | 43.64 |
| SrO | 0.18 |
| MgO | 6.17 |
| S | 1.25 |
| $TiO_2$ | 1.81 |
| BaO | 0.32 |
| $Al_2O_3$ | 9.16 |
| Cl | 0.02 |
| MnO | 1.96 |
| L.O.I. | 1.50 |
| $SiO_2$ | 31.10 |
| $K_2O$ | 1.11 |
| $Fe_2O_3$ | 1.17 |
| Total Sum | 100.00 |

As observed, addition of admixture was effective in improving the mechanical strength of specimens. This was true for 28- and 90-day cured samples, hence in good agreement with the published literature [74]. Upon increasing the curing time, the mechanical strength increased (Fig. 7-a and 7-b) mainly because the hydration reactions took place completely and thus, the final structure of the produced concrete would turn into a flawless structure [33]. It has been reported in previous studies that upon increasing the curing time of concrete samples containing graphene oxide, their compressive strength would also increase [106].

The admixture could effectively reduce the passing current in the conductivity test and enhance the concrete resistance to chloride penetration. According to Fig. 7-c, the lowest charge was passed in the concrete containing GGBFS and GO. High reduction was observed in the electrical conductivity from 4012 C to 1200 C for 90-day cured concrete containing GGBFS and GO. This observation that addition of admixture in 28 and 90 days cured samples could significantly decrease the charge conducted in Rapid Chloride Permeability tests (RCPTs) signifies increased resistance against chloride penetration (in Coulombs). Fig 7-d shows the Wenner test results from C2 samples that exhibit high surface electrical resistivity as well as the least electrical charge conduction (1200 to 2058 C) as a sign of high resistance to chloride ingress.

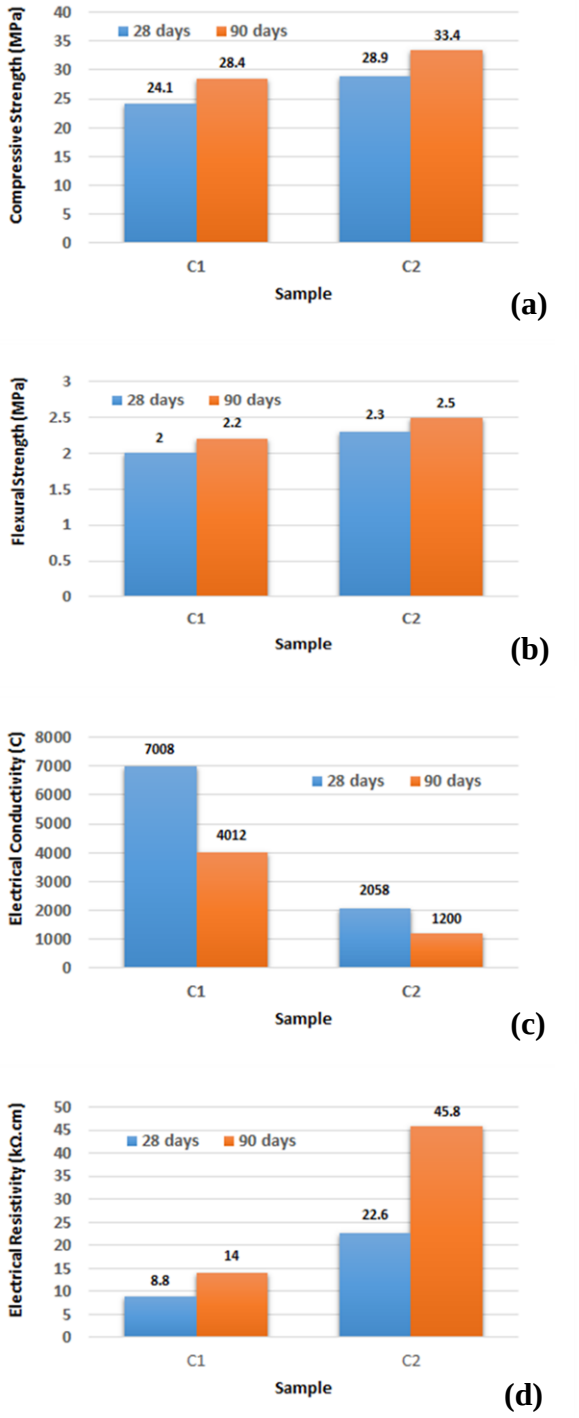


**Figure 7.** Mechanical and physical tests results of concrete samples at curing time 28-days and 90-days

ASTM 1202-12 Standard designates such charge conduction as low chloride permeability (Table 4). Electrical charge transfer during the RCPT was significantly declined in the concrete containing GGBFS and GO, thus confirming the positive role of GGBFS and GO in decreasing the chloride permeability and movement by immobilizing the free chloride.

**Table 4.** Chloride ion penetrability based on charge passed according to ASTM 1202-12 Standard

| The Charge Passed (C) | Chloride Ion Permeability |
|---|---|
| >4000 | High |
| 2000-4000 | Moderate |
| 1000-2000 | Low |
| 100-1000 | Very low |
| <100 | Negligible |

Fig. 8 shows the penetration of chloride ions in both ordinary concrete and that containing GGBFS and GO at the constant water temperature of 25 °C, constant time of 144, and pressures of 0.3, 0.5, and 0.7 MPa. In all experiments, upon increasing pressure, the penetration of chlorine ions into the ordinary concrete and that containing GGBFS and GO would increase. According to Fig. 8, water pressure is an important factor in the penetration of chlorine ions into the concrete. For example, at a pressure of 0.3 MPa, which is equivalent to 30 meters of water depth, penetration of chlorine ions into the concrete is less than 0.5 and 0.7 MPa. The direct effect of the water pressure on the penetration of chlorine ions has already been proven in other studies [82-85]. Equation (1) shows Fick's second law, where D is the diffusion coefficient, z the distance from the surface, C the chloride concentration, $C_s$ the surface concentration, and t the time (s).

$$C_{z,t} = C_s\left(1 - \mathrm{erf}\left(\frac{z}{2\sqrt{Dt}}\right)\right) \quad (1)$$

This equation makes it possible to derive concentration-dependent diffusion formulas and relate localized concentration to time [29,107]. The mechanism of the transfer of chloride ions under hydrostatic pressure is elaborated according to Fick's second law. In this study, the chloride diffusion coefficient in concrete was calculated using the least squares method and experimental data. Fig. 9 shows the diffusion coefficient of chloride ions in both ordinary concrete and that containing GGBFS and GO at the water temperature of 25 °C, time of 144 h, and pressures of 0.3, 0.5, and 0.7 MPa, respectively. According to this Figure, with an increase in the water pressure, the diffusion coefficient of chlorine ions in both types of concrete would increase. Based on these results, the highest diffusion coefficient of chlorine ion in both ordinary concrete and that containing GGBFS and GO is related to 0.7 MPa are $6.37\times10^{-11}$ $m^2/s$ and $5.78\times10^{-11}$ $m^2/s$, respectively. The lowest penetration coefficients related to 0.3 MPa are $3.18\times10^{-11}$ $m^2/s$ and $3.08\times10^{-11}$ $m^2/s$, respectively. Accordingly, upon increasing water pressure from 0.3 MPa to 0.7 MPa, the diffusion coefficient of chlorine ion in both ordinary concrete and that containing GGBFS and GO would increase up to 100 % and 87 %, respectively. The diffusion coefficient of chlorine ion in the concrete is shown in Fig. 10 at water temperatures of 25, 35, and 55 °C, respectively, and they are compared with each other. According to the results listed in this figure, the diffusion coefficient of chlorine ions is directly related to water temperature; in other words, it increases with an increase in the water temperature. This trend can be seen in both types of concrete. These results are consistent with those of the previous studies [72-77,108,109].

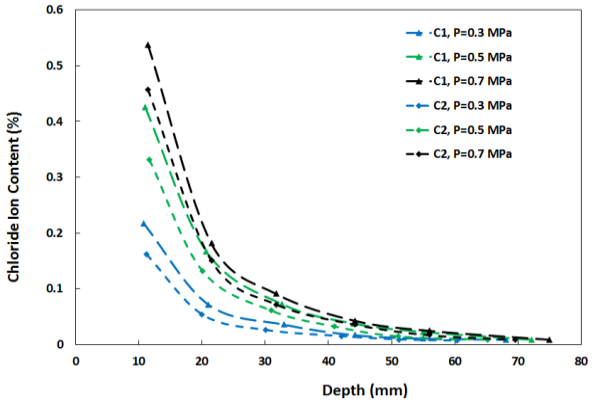


**Figure 8.** Profiles of chlorine ions penetration in Ordinary concrete(C1) and concrete containing GGBFS and GO (C2) at water temperature of 25 °C, time of 144 h and at pressures of 0.3, 0.5 and 0.7 MPa

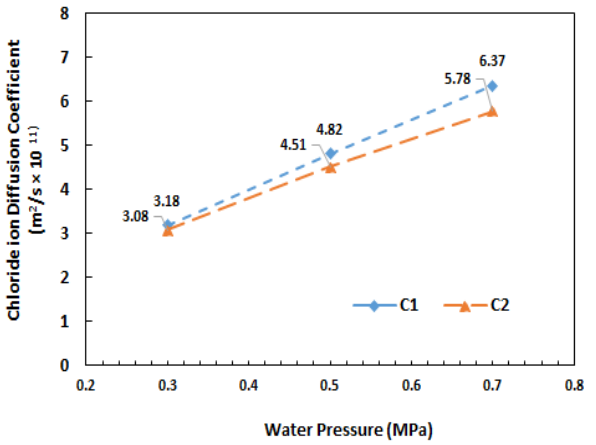


**Figure 9.** Chloride ion diffusion coefficient in both ordinary concrete (C1) and that containing GO and GGBFS (C2) at time of 144 hours, water temperature of 25 °C, and pressures of 0.3, 0.5, and 0.7 MPa

Fig. 10 shows the effects of pressure and temperature on the diffusion coefficient of chlorine ion in both ordinary concrete and that containing GGBFS and GO in 144 hours. According to the results from this figure, the diffusion coefficient of chlorine ion is directly related to pressure and temperature. On the contrary, the diffusion coefficient of chlorine ion in the concrete containing GGBFS and GO in all test cases is less than that in the ordinary concrete.

The main mechanism of chlorine ion transfer in the concrete at low pressures results from capillary adsorption. Increased chloride ion penetration caused by an increase in the pressure is indicative of a change in the chloride ion diffusion mechanism in a way that at high water pressures, the diffusion mechanism is considered the main mechanism for chlorine ion to enter the concrete in concrete [82,83]. A comparison of the the results in these two types of concrete in Figures 8-10 revealed that the concrete containing GGBFS and GO exhibited greater resistance to chlorine ion penetration. In addition, an increase in the chloride ion penetration resistance in this type of concrete is caused by an improvement in the pore structure [10,110-112]. Table 5 shows the physical structure characteristics of the tested concrete specimens, including ordinary concrete and that containing GGBFS and GO obtained from porosity test. Fig. 11 shows the pore size distribution in these two types of concrete used in this study. These results were obtained from the porosity test using mercury. This information includes the total amount of pores (more than 10 nm), small capillary pore volume, large capillary pore volume, and medium pore size (D50). Concrete has different pores in different sizes. The volume value of pores with different sizes occupies about one gram of cement paste that is called the pore size distribution [113].

Capillaries that are classified in two types are large capillary pores with a size of 50-1000 nm as well as small capillary pores with a size of 10-50 nm [102]. The average pore size equals 50 % of the cumulative volume of porosity that can indicate the pore size distribution [113]. According to Fig. 11, a comparison of the concrete containing GGBFS and GO with the ordinary one reveals that GGBFS can not only reduce the total porosity but also convert large capillary pores into small capillary pores. According to Table 5, in ordinary concrete, the volumes of large and small capillary pores are 33 and 18 ml/g, respectively; and in the concrete containing GGBFS and GO, these values are 16 and 30 ml/g, respectively. As a result of adding GO and GGBFS, the volume of small capillary pores increased, and that of large capillary pores decreased. According to these results, the average pore size in the concrete containing GGBFS and GO was considerbaly reduced compared to that in the concrete without additives. reduced compared to that in the concrete without additives. The average pore sizes in the concrete containing GGBFS and GO and ordinary concrete are 27 and 87 nm, respectively.

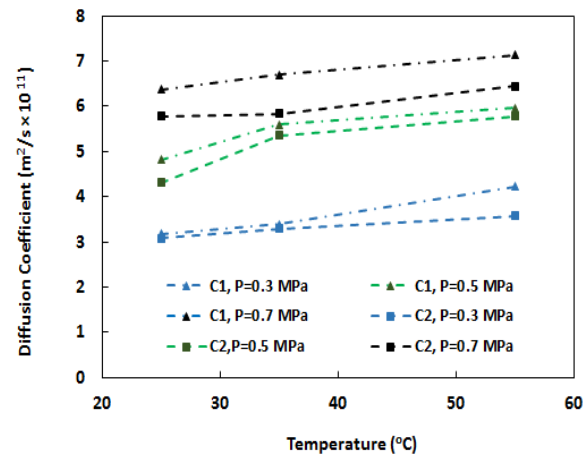


**Figure 10.** Chloride ion diffusion coefficient in Ordinary concrete (C1) and in concrete containing GO and GGBFS (C2) in 144 hours, at water temperatures of 25, 35, and 55 °C and at pressures of 0.3, 0.5, and 0.7 MPa

**Table 5.** Physical structures in ordinary concrete and concrete containing GO and GGBFS

| Sample Code | Large Porosity Volume (mL/gr) | Small Porosity Volume (mL/gr) | D50 (nm) | Porosity (%) |
|---|---|---|---|---|
| C1 | 33 | 18 | 87 | 13.1 |
| C2 | 16 | 30 | 27 | 11.1 |

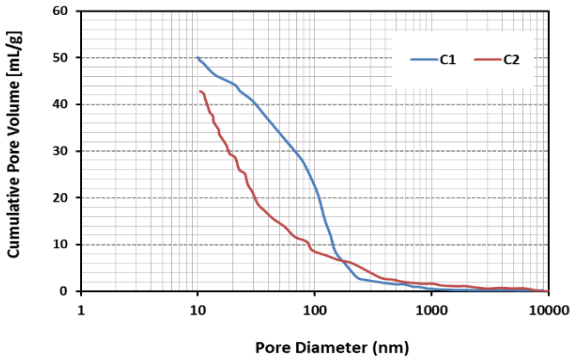


**Figure 11.** Comparison of pore size distributions in ordinary concrete (C1) and concrete containing GGBFS and GO (C2)

This reduction in porosity results the addition of GGBFS and GO, which causes more density in the samples. The effects of pozzolanic reaction in the concrete contributes to filling the pores and cracks and consequently, the concrete is compacted, and its resistance to chloride ion penetration is improved [105,113]. Fig. 12 shows the penetration of chloride ions in ordinary concrete and that containing GGBFS and GO at constant pressures of 0.7 MPa, constant water temperatures of 25 °C, and different times of 24, 72, and

144 hours repsectively. According to this figure, the concentration of the chloride ion increased over time in both ordinary concrete and that with GGBFS and GO additives. The concentration of chlorine ions in the concrete after 144 hours was much higher than that of chlorine ions in 24 hours and 72 hours in both types of concrete. According to this Figure, penetration of chlorine ion in the ordinary concrete sample at a depth of 10 mm from its surface of exposed to salt water containing chlorine ion for 144 hours is 2.2 times of that of the concrete sample for 24 hours. However, this difference was eliminated at greater depths. This behavior was also observed in the concrete containing GGBFS and GO sample.

In the environment of water pressure, chloride ion transfers to the internal parts mainly through convective motion caused by concentration diffusion and pressure infiltration [114-116]. The depth of capillary absorption and penetration is limited, and the convective region exists only within a certain depth beneath the surface of the concrete [115]. DuraCrete thought that the depth of influenced convection was 14 mm [116,117]. Lei concluded that the depth of a convection zone in an underground structure was approximately in the range of 5 mm-10 mm [118]. Within this depth, the chloride ion was transferred into the internal layer of the concrete under the action of the convection-diffusion coupling. In case the depth was greater than this value, the chloride ion transfer was mainly under the influence of diffusion [115-119]. Hence, the convection-diffusion coupling is the main machanism of the chloride ion transfer in the concrete used in this research. Fig. 13 shows the effect of time on the diffusion coefficient of chlorine ions in both ordinary concrete and that containing GGBFS and GO at a pressure of 0.7 MPa and ambient temperature. According to this figure, exposure time had a considerable effect on the diffusion coefficient of chlorine ions in concrete, and upon increasing the time, the diffusion coefficient of chlorine ions in concrete would decreases and become more stable over time. Of note, over time, the concentration of chlorine ions in the concrete increased much less than that in the concrete containing GGBFS and GO. Based on these results, the highest diffusion coefficient of chlorine ion in the ordinary concrete and that containing GGBFS and GO related to 24 hr are $22.8\times10^{-11}$ $m^2/s$ and $20.8\times10^{-11}$ $m^2/s$, respectively. The lowest penetration coefficients related to 144 hr are $6.37\times10^{-11}$ $m^2/s$ and $5.78\times10^{-11}$ $m^2/s$, respectively. Fig. 14 shows the effect of time and temperature on the diffusion coefficient of chlorine ion in both ordinary concrete and that containing GGBFS and GO at 0.7 MPa. According to this figure, the diffusion coefficient of chlorine ion is directly related to time and temperature. According to Fig. 14, upon increasing time in both types of concrete, the chlorine ion diffusion coefficient decreases, and upon increasing temperature, the chlorine ion penetration coefficient increases.

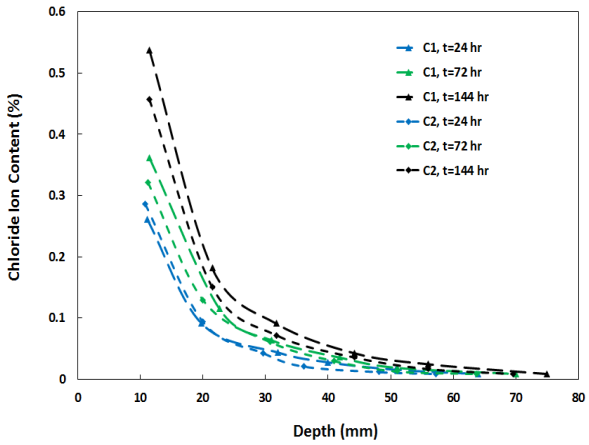


**Figure 12.** Profiles of chlorine ions penetration in ordinary concrete (C1) and concrete containing GGBFS and GO (C2) at constant water temperature of 25 °C, constant pressure of 0.7 MPa and at times of 24, 72, and 144 h

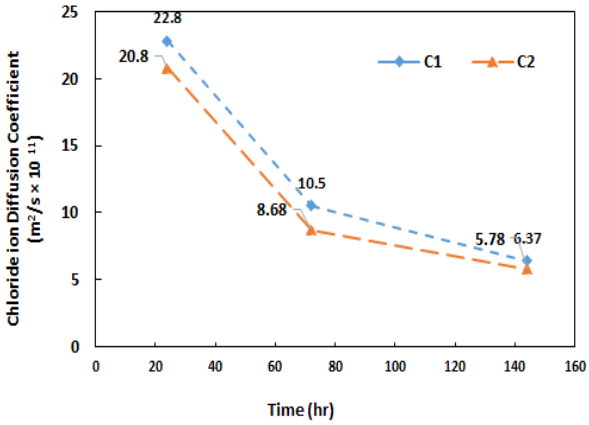


**Figure 13.** Chloride ion diffusion coefficient in ordinary concrete (C1) and in concrete containing GGBFS and GO (C2) at a pressure of 0.7 MPa, at water temperatures of 25 °C and at times of 24, 72, and 144 hours

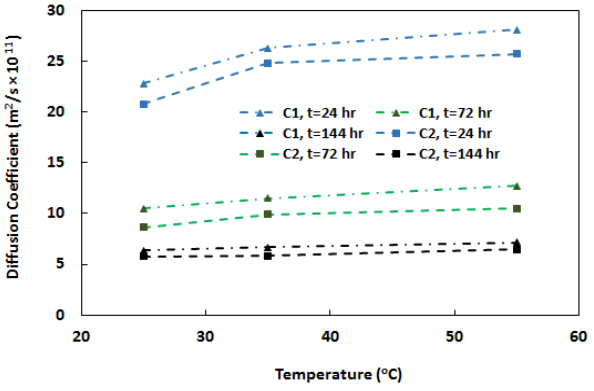


**Figure 14.** Chloride ion diffusion coefficient in ordinary concrete (C1) and in concrete containing GGBFS and GO (C2) at a pressure of 0.7 MPa, at water temperatures of 25, 35, and 55 °C and at times of 24, 72, and 144 hours

However, the diffusion coefficient of chlorine ion in concrete containing GGBFS and GO in all test cases is less than that of chlorine ion diffusion in ordinary concrete. According to the findings, water temperature also has a significant effect on the penetration of chlorine ions in concrete. Chloride ion penetrates significantly into both ordinary concrete and that containing GGBFS and GO at 55 °C, and this rate of change in ordinary concrete is greater than that of concrete containing GGBFS and GO mainly because the pores are filled with hydration products over time [120-123]. Sun et al. showed that when hydration reactions continued over time, the chloride concentration would increase, and the chloride diffusion coefficient would decrease with an increase in time at a certain depth [122].

Concrete containing GGBFS and GO exhibited the lowest penetration depth of chloride ion at a certain time. This difference was caused by the improvement of concrete structure due to the presence of GO and GGBFS during the test. On the contrary, the diffusion coefficient of chlorine ion in the concrete containing GGBFS and GO in all test cases was less than that of chlorine ion in concrete. In addition, according to Fig. 14, while the chlorine ion diffusion coefficient decreased upon increasing time, the value of decrease between 24 and 72 hours was greater than the that of decrease between 72 and 144 hours. This behavior was observed in both types of concrete with a main difference, i.e., the chlorine ion penetration coefficient in ordinary concrete samples was higher than that in the concrete containing GGBFS and GO. Therefore, it can be concluded that the microstructure of the concrete changes with time in different locations. Both chloride ion concentration and chloride diffusivity varied with time and space [122]. The coefficient of chloride diffusion decreased over time because the capillary pore structure was changed due to the continuous formation of hydration products, thus reaching a stable value [119,122].

Fig. 15 shows the diffusion coefficient of chloride ions in both ordinary concrete and that containing GGBFS and GO under different test conditions. As water pressure and temperature increased, the diffusion coefficient of chlorine ions in both types of concrete increased, too; however, upon increasing time, the diffusion coefficient of chlorine ions in both types of concrete would decrease. Based on these results, it can be concluded that the highest diffusion coefficient of chlorine ion in ordinary concrete and that containing GGBFS and GO observed at 0.7 MPa, one-day time (24 hr), and 55 °C are $28.1\times10^{-11}$ $m^2/s$ and $25.7\times10^{-11}$ $m^2/s$, respectively. The lowest penetration coefficients related to 0.3 MPa, six-day time (144 hr) and 25 °C are $3.18\times10^{-11}$ $m^2/s$ and $3.08\times10^{-11}$ $m^2/s$, respectively. The mix with 0.1 wt. % GO and 50 wt. % GGBFS showed considerable performance in terms of diffusion. The results revealed that addition of 0.1 wt. % graphene oxide and 50 wt. % granular slag decreased the chloride penetration in the concrete sample up to 17.6 % during 90 days compared to ordinary concrete sample. Table 6 lists the values of D in different concrete samples were obtained through Equation (2) by other researchers and compares them with the results from this research [85, 124-139]. According to this table, the values of D in different concrete samples in this study are the same as those previously obtaiened by other researchers.

In order to further investigate the microstructure of concrete specimens, Fig. 16 depicts the SEM images of ordinary and concrete containing GO and GGBFS after 90-day curing time. As can be clearly seen obviously, after addition of GO and GGBFS, the structural porosity of the concrete was significantly reduced, hence a dense structure.

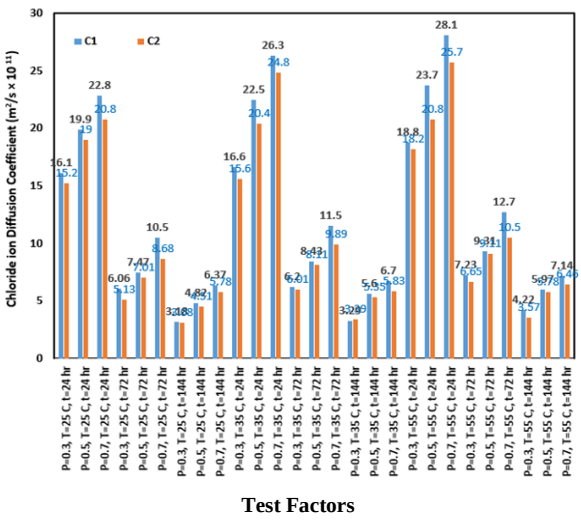


**Figure 15.** Chloride ion diffusion coefficient in ordinary concrete and in concrete containing GGBFS and GO under different experiments

**Table 6.** Chloride diffusion coefficient values in ordinary concretes obtained from some other studies and this study

| Maximum Exposure Time (Day) | D ($m^2/s$) | Reference |
|---|---|---|
| 1 | 5E-11 | [85] |
| 108 | 1E-10 | [124] |
| 10 | 8E-12 | [125] |
| 1 | 1E-11 | [126] |
| 30 | 1E-11 | [127] |
| 28 | 2E-11 | [128] |
| 1022 | 5E-12 | [129] |
| 25 | 6E-11 | [130] |
| 365 | 6E-12 | [131] |
| 5 | 9E-12 | [132] |
| 240 | 1E-12 | [133] |
| 180 | 3E-11 | [134] |
| 28 | 2E-11 | [135] |
| 30 | 3E-11 | [136] |
| 100 | 5E-12 | [137] |
| 30 | 1E-12 | [138] |
| 60 | 7E-12 | [139] |
| 6 | 3E-11 to 2E-10 | This Paper |

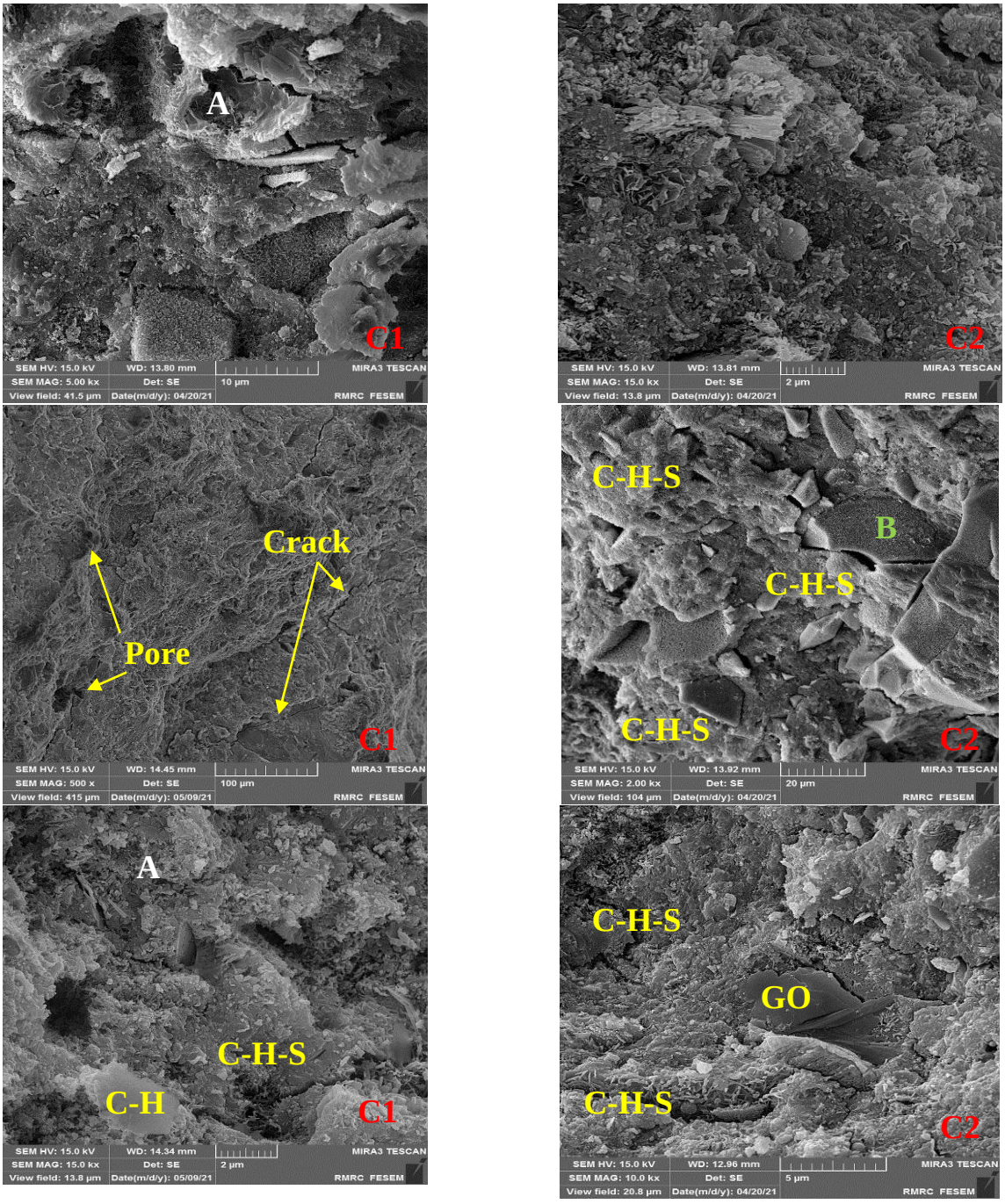


**Figure 16.** Comparison of pore size distributions in ordinary concrete (C1) and concrete containing GGBFS and GO (C2)

In typical concrete specimens, the microstructure is generally composed of C-H calcium hydroxide plate crystals and hydrated needle-shaped compounds along with hydrated calcium silicate compounds C-H-S. All of these compounds are formed in the concrete structure as a result of initial reactions between cement and water in the hydration process. The initial reaction of cement and water in the hydration process is as follows [61,99]:

$$2(3CaO\cdot SiO_2) + 6H_2O \rightarrow \underset{\text{(Primary C–S–H)}}{3CaO\cdot 2SiO_2\cdot 3H_2O} + \underset{}{3Ca(OH)_2} \quad (2)$$

In the presence of granular slag, activated $SiO_2$ can react with high-purity calcium hydroxide and calcium silicate hydrate to make hydrated calcium silicate more stable. At the same time, activated $Al_2O_3$ can react with

calcium hydroxide to produce hydrated calcium aluminate. The main reaction is as follows [105,113].

$$3Ca(OH)_2 + Slag + H_2O \rightarrow 3CaO{\cdot}2SiO_2{\cdot}3H_2O + \text{(Secondary C–S–H)} \quad 4CaO{\cdot}Al_2O_3{\cdot}3H_2O \text{ (Secondary C–A–H)} \quad (3)$$

As a result, secondary reactions of calcium hydroxide (C-H) crystals in the presence of slag are converted to C-H-S, and this combination leads to more filling of cavities and structural pores [105,113].

The microstructure of the ordinary concrete specimens is largely composed of needle-shaped grains and plate as well as hexagonal crystals of calcium hydroxide C-H. Despite the formation of some hydrated silicon compounds in them, their amount was negligible enough to affect the porosity of the concrete structure. Fig. 16 shows the areas with folded plate morphology of graphene oxide sheets. The analysis of elements from points A and B shown in the microstructural images of the concrete containing GGBFS and GO specimens are shown in Fig. 17. According to the results in Fig. 17, addition of slag and graphene oxide to the concrete led to the formation of these secondary compounds with a lower Ca-to-Si ratio, which is about two in ordinary cement. However, with the formation of these compounds, i.e., hydrated calcium silicate, in many parts of the cementitious background, this ratio would decrease by 1.4 [140-142].

Slag contains higher amounts of aluminum, silicon and magnesium, which leads to the formation of hydrotalacite, resulting in the replacement of silicon by aluminum in C-S-H and reducing their C/S ratio less than Portland cement in concrete [142].

The interactions among pressure, time, and temperature as well as their effect on the concentration of chlorine ion in both ordinary concrete and that containing GGBFS and GO at a depth of 20 ± 1 mm from the surface of the sample exposed to water containing chlorine ion are shown as a three-dimensional diagram and Pareto

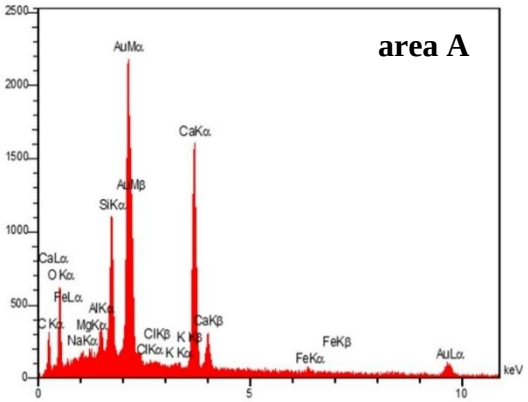


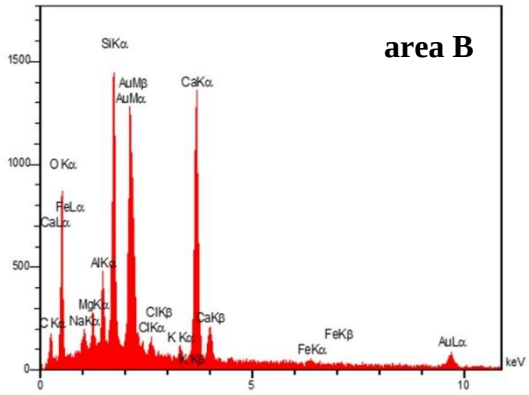


**Figure 17.** Analysis of point elements in microstructural images of ordinary concrete (area A) and concrete containing GGBFS and GO (area B)

diagram in Fig. 18 and Fig. 19, respectively. The Pareto diagram shows the absolute values of the standardized effects listed hierarchically from the maximum to the minimum. The diagram also draws a reference line to determine which effects are statistically significant. The reference line for statistical significance depends on the level of significance (indicated by α). According to Fig. 18, pressure has a greater effect on chlorine ion penetration than other parameters. After pressure, time is the most important factor, and temperature is the third one. In the next positions in terms of their simportamce are the interaction between pressure and time as well as concrete composition. Fig. 19 shows the sequence of factors affecting the release of chlorine ions in the concrete used in this study. All factors that cross the reference line (2.31) are statistically significant. The order of the effective effects of the evaluated parameters is also shown in this Figure. According to these results indicate, the level of significance for each evaluated response is different from the other. These results also indicated that the level of significance for each evaluated response is different from the other. According to Fig. 19, the intensity of the effect of different parameters on the amount and chlorine ion diffusion in concrete is as follows:

1- Water pressure
2- Exposed time
3- Water temperature
4- Interaction of water pressure - exposed time
5- Concrete composition

The cost of casting the mixed designed were estimated and reported in Tables 7 and 8. The cost of concrete composites was estimated using the commercialized market prices of the materials. The economic index for strength (compressive strength/cost per $m^3$) was observed to have same value at concrete containing GGBFS and GO compare to ordinary concrete but the economic Index for electrical conductivity (electrical conductivity/cost per $m^3$) shows that concrete containing GGBFS and GO

is a better mix than the ordinary concrete in terms of chlorine ion permeability and economy. Table 8 reveals that the cost of materials for making concrete containing GGBFS and GO sample is 24.5 % higher than this cost for ordinary concrete; however, given the economic index for electrical conductivity, using this mix is cost-effective.

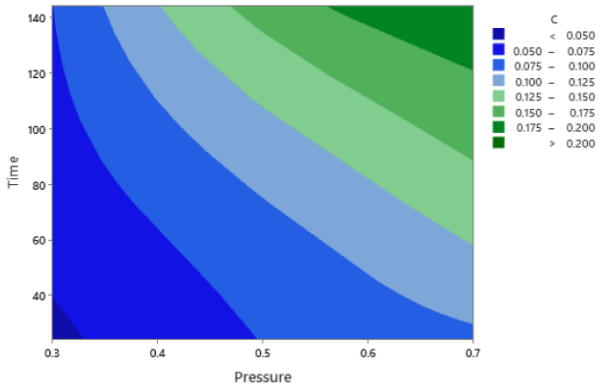


**(a) Influence of Pressure and Time**

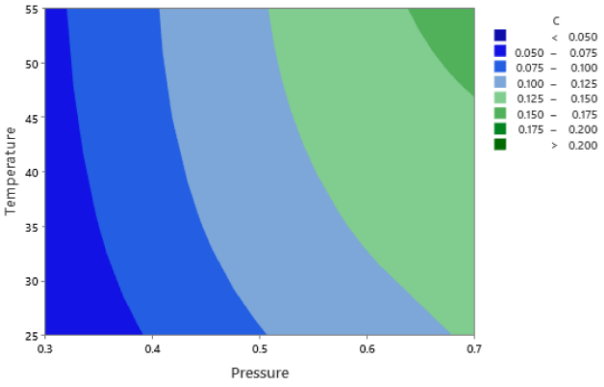


**(b) Influence of Pressure and Temperature**

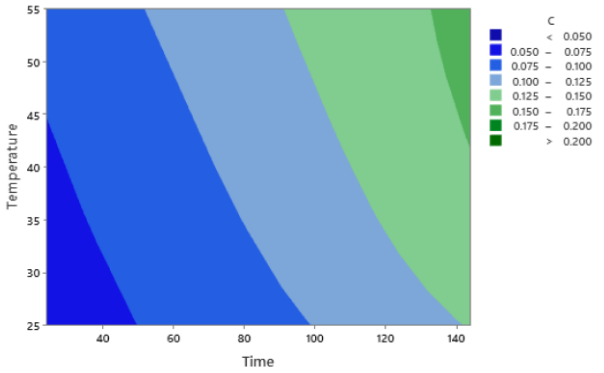


**(c) Influence of Time and Temperature**

**Figure 18.** The interactions of time, temperature and pressure on the chloride content in ordinary concrete and concrete containing GGBFS and GO at a depth of 20 ± 1 mm

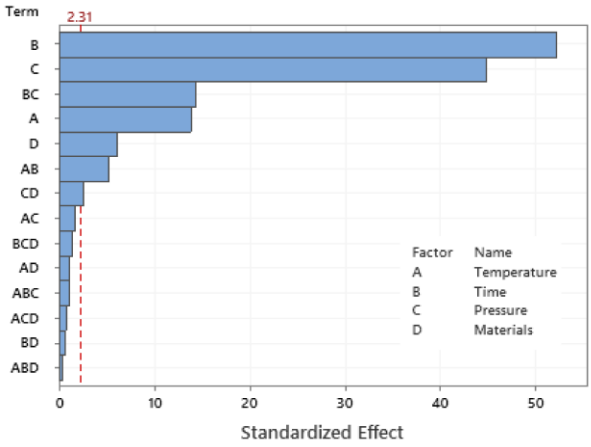


**Figure 19.** Effect of time, temperature and pressure and their interactions on the concentration of chlorine ions in concrete

**Table 7.** Cost of materials

| Materials | Cost ( USD/kg) |
|---|---|
| OPC | 0.1 |
| GO | 0.02 |
| GGBFS | 0.15 |
| Water | 0.0007 |
| Fine Aggregate | 0.02 |
| Coarse Aggregate | 0.013 |
| SP | 1.6 |

 OPC: Ordinary Portland Cement, GO: Graphene Oxide, GGBFS: Ground Granulated Blast Furnace Slag, SP: (Carboxylate based) Super Plasticizer

**Table 8.** Cost analysis of mixes per $m^3$ of concrete

| Mix | C1 (Ordinary Concrete) | C2 (Concrete Containing GGBFS and GO) |
|---|---|---|
| Compressive Strength (MPa) | 28.4 | 33.4 |
| Electrical Conductivity (C) | 4012 | 1200 |
| Cost of GGBFS (USD) | 0 | 31.875 |
| Cost of GO (USD) | 0 | 6.936 |
| Cost of OPC (USD) | 42.5 | 21.25 |
| Cost of water (USD) | 0.119 | 0.119 |
| Cost of Fine Aggregate (USD) | 20.11 | 20.11 |
| Cost of Coarse Aggregate (USD) | 8.794 | 8.794 |
| Cost of Super Plasticizer (USD) | 0.068 | 0.068 |
| Total Cost (USD) | 71.591 | 89.152 |
| Economic Index for Strength | 0.397 | 0.375 |
| Economic Index for Electrical Conductivity | 56.040 | 13.460 |

## 4. CONCLUSIONS

Throughout this study, the following concluding remarks were made:

1. Addition of 0.1 wt. % graphene oxide and 50 wt. % granular slag increased the compressive strength of concrete sample upto 19.9 % during 28 days and 17.6 % during 90 days compared to ordinary concrete sample. Concrete with a combination of 0.1 wt. % graphene oxide and 50 wt. % granular slag exhibited an increase in the flexural strength of 15 % during 28 days of curing and 13.6 % during 90 days of curing.
2. High reduction in electrical conductivity from 4012C to 1200C was observed for 90-day cured samples containing 0.1 wt. % GO and 50 wt. % GGBFS compared to the ordinary sample. Addition of 0.1 wt. % GO and 50 wt. % GGBFS led to the highest surface electrical resistivity and the least electrical charge conduction, a sign of high resistance to chloride ingress and this mix is cost-effective.
3. The penetration of chlorine ions into ordinary concrete and concrete containing GGBFS and GO concrete increasedsignificantly upon increasing water pressure and temperature. The mix with 0.1 wt. % GO and 50 wt. % GGBFS exhibited considerable performance in the case of chloride penetration in the concrete. This admixure reduced the chloride penetration by 17.6 % in 90 days compared to ordinary concrete.
4. The convection-diffusion coupling is the main mechanism of the transfer of chloride ion in concrete in this research.
5. Increasing resistance to chloride ion penetration in the concrete containing GGBFS and GO was caused by the improvement of pore structure and increase in concrete density. Due to the filling of pores and cracks, concrete becomes denser and its resistance to chloride ion penetration was improved.
6. UPon increasing water pressure and tempertature, the diffusion coefficient of chlorine ions in both types of concrete increased; however, an increase in time reduced the coefficient mainly because the capillary pore structure was changed due to the continuous formation of hydration products, thus reaching a stable value over time.
7. The order of the effect of the studied parameters on the amount and intensity of chlorine ion emission in concrete, respectively: 1) water pressure, 2) exposure time, 3) water temperature, 4) water pressure interaction - exposure time, and 5) concrete composition.

## ACKNOWLEDGEMENTS

The authors appreciatively acknowledge the Research Council of Shahid Bahonar University.

## NOMENCLATURE

| | |
|---|---|
| C | Chloride Concentration |
| Cs | Surface Concentration |
| D | Diffusion Coefficient |
| erf | Error Function |
| t | Time |
| x | Distance |

## REFERENCES

1. Shen, D., Jiao, Y., Kang, J., Feng, Z., Shen, Y., "Influence of ground granulated blast furnace slag on early-age cracking potential of internally cured high performance concrete", ***Construction and Building Materials***, Vol. 233, (2020), 117083. https://doi.org/10.1016/j.conbuildmat.2019.117083
2. Qu, F., Li, W., Dong, W., Tam, V. W., Yu, T., "Durability deterioration of concrete under marine environment from material to structure: A critical review", ***Journal of Building Engineering***, Vol. 35, (2021), 102074. https://doi.org/10.1016/j.jobe.2020.102074
3. Khan M. U., Ahmad, S., Al-Gahtani, H. J. "Chloride-induced corrosion of steel in concrete: an overview on chloride diffusion and prediction of corrosion initiation time", ***International Journal of Corrosion***, Vol. 2017, (2017), 5819202. https://doi.org/10.1155/2017/5819202
4. Neville, A., "Chloride attack of reinforced concrete: an overview", ***Materials and Structures***, Vol. 28, No. 2, (1995), 63-70. https://doi.org/10.1007/BF02473172
5. Kassir, M. K, Ghosn, M., "Chloride-induced corrosion of reinforced concrete bridge decks", ***Cement and Concrete Research***, Vol. 32, No. 1, (2002), 139-143. https://doi.org/10.1016/S0008-8846(01)00644-5
6. Khameneh Asl, S., Sadeghian, A., "Strength and Toughness of Reinforced Concrete with Coated Steel Fibers", ***Advanced Ceramics Progress***, Vol. 5, No. 1, (2019), 9-14. https://doi.org/10.30501/ACP.2019.93125
7. Ding, J. T., Li, Z., "Effects of metakaolin and silica fume on properties of concrete", ***ACI Materials Journal***, Vol. 99, No. 4, (2002), 393-398. http://hdl.handle.net/1783.1/23320
8. Ferreira, R. M., Castro-Gomes, J. P., Costa, P., Malheiro, R., "Effect of metakaolin on the chloride ingress properties of concrete", ***KSCE Journal of Civil Engineering***, Vol. 20, No. 4, (2016), 1375-1384. https://doi.org/10.1007/s12205-015-0131-8
9. Yoo, S. W., Kwon, S. J., "Effects of cold joint and loading conditions on chloride diffusion in concrete containing GGBFS", ***Construction and Building Materials***, Vol. 115, (2016), 247-255. https://doi.org/10.1016/j.conbuildmat.2016.04.010
10. Park, J. S., Yoon, Y. S., Kwon, S. J., "Strength and Resistance to chloride penetration in concrete containing GGBFS with ages", ***Journal of the Korea Concrete Institute***, Vol. 29, No. 3, (2017), 307-314. https://doi.org/10.4334/JKCI.2017.29.3.307
11. Du, H., Gao, H. J., Dai Pang, S., "Improvement in concrete resistance against water and chloride ingress by adding graphene nanoplatelet", ***Cement and Concrete Research***, Vol. 83, (2016), 114-123. https://doi.org/10.1016/j.cemconres.2016.02.005
12. Wu, Z., Shi, C., Khayat, K. H., "Influence of silica fume content on microstructure development and bond to steel fiber in ultra-high strength cement-based materials (UHSC)", ***Cement and Concrete Composites***, Vol. 71, (2016), 97-109. https://doi.org/10.1016/j.cemconcomp.2016.05.005
13. Samad, S., Shah, A., Limbachiya, M. C., "Strength development characteristics of concrete produced with blended cement using ground granulated blast furnace slag (GGBS) under various curing conditions", ***Sādhanā***, Vol. 42, No. 7, (2017), 1203-1213. https://doi.org/10.1007/s12046-017-0667-z

14. Gesoğlu, M., Özbay, E., "Effects of mineral admixtures on fresh and hardened properties of self-compacting concretes: binary, ternary and quaternary systems", ***Materials and Structures***, Vol. 40, No. 9, (2007), 923-937. https://doi.org/10.1617/s11527-007-9242-0
15. Özbay, E., Erdemir, M., Durmuş, H. İ., "Utilization and efficiency of ground granulated blast furnace slag on concrete properties–A review", ***Construction and Building Materials***, Vol. 105, (2016), 423-434. https://doi.org/10.1016/j.conbuildmat.2015.12.153
16. Ying, J., Zhou, B., Xiao J., "Pore structure and chloride diffusivity of recycled aggregate concrete with nano-$SiO_2$ and nano-$TiO_2$", ***Construction and Building Materials***, Vol. 150, (2017), 49–55. https://doi.org/10.1016/j.conbuildmat.2017.05.168
17. Ying, J., Xiao, J., Tam, V. W., "On the variability of chloride diffusion in modelled recycled aggregate concrete", ***Construction and Building Materials***, Vol. 41, (2013), 732–741. https://doi.org/10.1016/j.conbuildmat.2012.12.031
18. Wang, H., Hou, P., Li, Q., Adu-Amankwah, S., Chen, H., Xie, N., Zhao, P., Huang, Y., Wang, S., Cheng, X., "Synergistic effects of supplementary cementitious materials in limestone and calcined clay-replaced slag cement", ***Construction and Building Materials***, Vol. 282, (2021), 122648. https://doi.org/10.1016/j.conbuildmat.2021.122648
19. Xiao, B., Wen, Z., Miao, S., Gao, Q., "Utilization of steel slag for cemented tailings backfill: Hydration, strength, pore structure, and cost analysis", ***Case Studies in Construction Materials***, Vol. 15, (2021), e00621. https://doi.org/10.1016/j.cscm.2021.e00621
20. Teng, S., Lim, T. Y. D., Divsholi, B. S., "Durability and mechanical properties of high strength concrete incorporating ultra fine Ground Granulated Blast-furnace Slag", ***Construction and Building Materials***, Vol. 40, (2013), 875–881. http://doi.org/10.1016/j.conbuildmat.2012.11.052
21. Sideris, K. K., Tassos, C., Chatzopoulos, A., Manita, P., "Mechanical characteristics and durability of self compacting concretes produced with ladle furnace slag", ***Construction and Building Materials***, Vol. 170, (2018), 660–667. https://doi.org/10.1016/j.conbuildmat.2018.03.091
22. Chen, W., Zhu, H., He, Z., Yang, L., Zhao, L. Wen, C., "Experimental investigation on chloride-ion penetration resistance of slag containing fiber-reinforced concrete under drying-wetting cycles", ***Construction and Building Materials***, Vol 274, (2021), 121829. https://doi.org/10.1016/j.conbuildmat.2020.121829
23. Ali-Boucetta, T., Behim, M., Cassagnabere, F., Mouret, M., Ayat, A., Laifa, W., "Durability of concrete containing GGBFS and GO containing waste bottle glass and granulated slag", ***Construction and Building Materials***, Vol. 270, (2021), 121133. https://doi.org/10.1016/j.conbuildmat.2020.121133
24. Fan, J., Zhu, H., Shi, J., Li, Z., Yang, S., "Influence of slag content on the bond strength, chloride penetration resistance, and interface phase evolution of concrete repaired with alkali activated slag/fly ash", ***Construction and Building Materials***, Vol. 263, (2020), 120639. https://doi.org/10.1016/j.conbuildmat.2020.120639
25. Shi, H. S., Xu, B. W., Zhou, X. C., "Influence of mineral admixtures on compressive strength, gas permeability and carbonation of high performance concrete", ***Construction and Building Materials***, Vol 23, Vol. 5, (2009), 1980-1985. https://doi.org/10.1016/j.conbuildmat.2008.08.021
26. Zhuang S., Wang, Q., "Inhibition mechanisms of steel slag on the early-age hydration of cement", ***Cement and Concrete Research***, Val. 140, (2021), 106283. https://doi.org/10.1016/j.cemconres.2020.106283
27. Gencel, O., Karadag, O., Oren, O. H., Bilir, T., "Steel slag and its applications in cement and concrete technology: A review", ***Construction and Building Materials***, Vol. 283, (2021), 122783. https://doi.org/10.1016/j.conbuildmat.2021.122783
28. Zheng, D., Yang, H., Yu, F., Zhang, B., Cui, H., "Effect of graphene oxide on the crystallization of calcium carbonate by $C_3S$ carbonation", ***Materials***, Vol. 12, No. 13, (2019), 2045. https://doi.org/10.3390/ma12132045
29. Jiang, Y., Ling, T., Shi, C., Pan. S, "Characteristics of steel slags and their use in cement and concrete—A review", ***Resources, Conservation and Recycling***, Vol. 136, (2018), 187-197. https://doi.org/10.1016/j.resconrec.2018.04.023
30. Ramezanianpour, A. A., Malhotra, V. M., "Effect of curing on the compressive strength, resistance to chloride-ion penetration and porosity of concretes incorporating slag, fly ash or silica fume", ***Cement and Concrete Composites***, Vol. 17, No. 2, (1995), 125–133. https://doi.org/10.1016/0958-9465(95)00005-W
31. Bagheri, A. R., Zanganeh, H., Moalemi, M. M., "Mechanical and durability properties of ternary concretes containing silica fume and low reactivity blast furnace slag", ***Cement and Concrete Composites***, Vol. 34, No. 5, (2012), 663–670. https://doi.org/10.1016/j.cemconcomp.2012.01.007
32. Jau, W. C., Tsay, D. S., "A study of the basic engineering properties of slag cement concrete and its resistance to seawater corrosion", ***Cement and Concrete Research***, Vol. 28, No. 10, (1998), 1363–1371. https://doi.org/10.1016/S0008-8846(98)00117-3
33. Hadj-sadok, A., Kenai, S., Courard, L., Darimont, A., "Microstructure and durability of moratrs modified with medium active blast furnace slag", ***Construction and Building. Materials***, Vol. 25, No. 2, (2011), 1018–1025. https://doi.org/10.1016/j.conbuildmat.2010.06.077
34. Sengul, O., Tasdemir, M. A., "Compressive strength and rapid chloride permeability of concretes with ground fly ash and slag", ***Journal of Materials in Civil Engineering***, Vol. 21, No. 9, (2009), 494–501. https://doi.org/10.1061/(ASCE)0899-1561(2009)21:9(494)
35. Kayali, O., Khan, M. S. H., Sharfuddin Ahmed, M., "The role of hydrotalcite in chloride binding and corrosion protection in concretes with ground granulated blast furnace slag", ***Cement and Concrete Composites***, Vol. 34, No. 8, (2012), 936–945. https://doi.org/10.1016/j.cemconcomp.2012.04.009
36. Yeau, K. Y., Kim, E. K., "An experimental study on corrosion resistance of concrete with ground granulate blast-furnace slag", ***Cement and Concrete Research***, Vol. 35, No. 7, (2005), 1391–1399. https://doi.org/10.1016/j.cemconres.2004.11.010
37. Cheng, A., Huang, R., Wu, J. K., Chen, C. H., "Influence of GGBS on durability and corrosion behavior of reinforced concrete", ***Materials Chemistry and Physics***, Vol. 93, No. 2-3, (2005), 404–411. https://doi.org/10.1016/j.matchemphys.2005.03.043
38. Gupta, S., "Effect of content and fineness of slag as high volume cement replacement on strength and durability of ultra-high performance mortar", ***Journal of Building Materials and Structures***, Vol. 3, No. 2, (2016), 43–54. https://doi.org/10.5281/zenodo.242626
39. Dhir, R. K., El-Mohr, M. A. K., Dyer, T. D., "Chloride binding in GGBS concrete", ***Cement and Concrete Research***, Vol. 26, No. 12, (1996), 1767–1773. https://doi.org/10.1016/S0008-8846(96)00180-9
40. Berndt, M. L., "Properties of sustainable concrete containing fly ash, slag and recycled concrete", ***Construction and Building Materials***, Vol. 23, No. 7, (2009), 2606–2613. https://doi.org/10.1016/j.conbuildmat.2009.02.011
41. Thomas, M. D., Scott, A., Bremner, T., Bilodeau, A., Day, D., "Performance of slag concrete in marine environment", ***ACI Materials Journal***, Vol. 105, No. 6, (2008), 628–634. https://doi.org/10.14359/20205
42. Mo, K. H., Alengaram, U. J., Jumaat, M. Z., Yap, S. P., "Feasibility study of high volume slag as cement replacement for sustainable structural lightweight oil palm concrete", ***Journal of Cleaner Production***, Vol. 91, (2015), 297–304. https://doi.org/10.1016/j.jclepro.2014.12.021
43. Gesoğlu, M., Güneyisi, E., Özbay, E., "Properties of self compacting concretes made with binary, ternary, and quaternary cementitious blends of fly ash, blast furnace slag, and silica fume", ***Construction and Building Materials***, Vol. 23, No. 5, (2009), 1847–1854. https://doi.org/10.1016/j.conbuildmat.2008.09.015

44. Aly, T., Sanjayan, J. G., "Mechanism of early shrinkage of concretes", ***Materials and Structures***, Vol. 42, No. 4, (2009), 461–468. https://doi.org/10.1617/s11527-008-9394-6
45. Elahi, A., Basheer, P. A. M., Nanukuttan, S. V., Khan, Q. U. Z., "Mechanical and durability properties of high performance concretes containing supplementary cementitious materials", ***Construction and Building Materials***, Vol. 24, No. 3, (2010), 292–299. https://doi.org/10.1016/j.conbuildmat.2009.08.045
46. McNally, C., Sheils, E., "Probability-based assessment of the durability characteristics of concretes manufactured using CEM II and GGBS binders", ***Construction and Building Materials***, Vol. 30, (2012), 22–29. https://doi.org/10.1016/j.conbuildmat.2011.11.029
47. Aprianti, E., Shafigh, P., Zawawi, R., Abu Hassan, Z. F., "Introducing an effective curing method for mortar containing high volume cementitious materials", ***Construction and Building Materials***, Vol. 107, (2016), 365–377. https://doi.org/10.1016/j.conbuildmat.2015.12.100
48. Nazari, A., Riahi, S., "Microstructural, thermal, physical and mechanical behavior of the self compacting concrete containing $SiO_2$ nanoparticles", ***Materials Science and Engineering A***, Vol. 527, No. 29-30, (2010), 7663-7672. https://doi.org/10.1016/j.msea.2010.08.095
49. Nazari, A., Riahi, S., "Effects of CuO nanoparticles on compressive strength of self-compacting concrete", ***Sadhana***, Vol. 36, No. 3, (2011), 371–391. https://doi.org/10.1007/s12046-011-0023-7
50. Nazari, A., Riahi S., "The role of $SiO_2$ nanoparticles and ground granulated blast furnace slag admixtures on physical, thermal and mechanical properties of self compacting concrete", ***Materials Science and Engeering: A***, Vol. 528, No. 4-5, (2011), 2149–2157. https://doi.org/10.1016/j.msea.2010.11.064
51. Nazari, A., Riahi, S., "The effects of $TiO_2$ nanoparticles on physical, thermal and mechanical properties of concrete using ground granulated blast furnace slag as binder", ***Materials Science and Engeering: A***, Vol. 528, No. 4-5, (2011), 2085–2092. https://doi.org/10.1016/j.msea.2010.11.070
52. Nazari, A., Riahi, S., "The effects of $ZrO_2$ nanoparticles on physical and mechanical properties of high strength self compacting concrete", ***Materials Research***, Vol. 13, No. 4, (2010), 551-556. https://doi.org/10.1590/S1516-14392010000400019
53. Nazari, A., Riahi, S., "The effects of $ZnO_2$ nanoparticles on properties of concrete using ground granulated blast furnace slag as binder", ***Materials Research***, Vol. 14, No. 3, (2011), 299–306. https://doi.org/10.1590/S1516-14392011005000052
54. Megat Johari, M. A., Brooks, J. J., Kabir, S., Rivard, P., "Influence of supplementary cementitious materials on engineering properties of high strength concrete", ***Construction and Building Materials***, Vol. 25, No. 5, (2011), 2639–2648. https://doi.org/10.1016/j.conbuildmat.2010.12.013
55. Lyu, S. H., Sun, T., Liu, J. J., Ma, Y. J., Qiu, C. C., "Toughening effect and mechanism of graphene oxide nanosheets on cement matrix composites", ***Acta Materiae Compositae Sinica***, Vol. 31, No. 3, (2014), 644-652. https://fhclxb.buaa.edu.cn/en/article/id/12119
56. Mohammed, A., Sanjayan, J. G., Duan, W. H., Nazari, A., "Graphene oxide impact on hardened cement expressed in enhanced freeze-thaw resistance", ***Journal of Materials in Civil Engineering***, Vol. 28, No. 9, (2016), 04016072. https://doi.org/10.1061/(ASCE)MT.1943-5533.0001586
57. Yuan, X. Y., Zeng, J. J., Niu, J. W., Qin, Z., "Effect of different water-reducing agents on mechanical properties and microstructure of graphite oxide-blended cement mortar", ***Journal of Functional Materials***, Vol. 49, No. 10, (2018), 10184-10189. https://doi.org/10.3969/j.issn.1001-9731.2018.10.032
58. Devasena, M., Karthikeyan, J., "Investigation on strength properties of Graphene Oxide Concrete", ***International Journal of Engineering Science Invention Research & Development***, Vol. 1, No. 8, (2015), 307-310. https://citeseerx.ist.psu.edu/viewdoc/download?doi=10.1.1.1082.3858&rep=rep1&type=pdf
59. Wang, Q., Wang, J., Lu, C. X., Liu, B. W., Zhang, K., Li, C. Z., "Influence of graphene oxide additions on the microstructure and mechanical strength of cement", ***New Carbon Materials***, Vol. 30, No. 4, (2015), 349-356. https://doi.org/10.1016/S1872-5805(15)60194-9
60. Lua, Z., Li, X., Hanif, A., Chen, B., Parthasarathy, P., Yu, J., Li, Z., "Early-age interaction mechanism between the graphene oxide and cement hydrates", ***Construction and Building Materials***, Vol. 152, (2017), 232-239. https://doi.org/10.1016/j.conbuildmat.2017.06.176
61. Hou, D., Lu, Z., Li, X., Ma, H., Li, Z., "Reactive molecular dynamics and experimental study of graphene-cement composites: Structure, dynamics and reinforcement mechanisms", ***Carbon***, Vol. 115, (2017), 188-208. https://doi.org/10.1016/j.carbon.2017.01.013
62. Long, W. J., Wei, J. J., Xing, F., Khayat, K. H., "Enhanced dynamic mechanical properties of cement paste modified with graphene oxide nanosheets and its reinforcing mechanism", ***Cement and Concrete Composites***, Vol. 93, (2018), 127-139. https://doi.org/10.1016/j.cemconcomp.2018.07.001
63. Wang, Q., Li, S., Pan, S., Cui, X., Corr, D. J., Shah, S. P., "Effect of graphene oxide on the hydration and microstructure of fly ash-cement system", ***Construction and Building Materials***, Vol. 198, (2019), 106-119. https://doi.org/10.1016/j.conbuildmat.2018.11.199
64. Yang, H., Monasterio, M., Cui, H., Han, N., "Experimental study of the effects of graphene oxide on microstructure and properties of cement paste composite", ***Composites Part A: Applied Science and Manufacturing***, Vol. 102, (2017), 263-272. https://doi.org/10.1016/j.compositesa.2017.07.022
65. Liu, Q., Wu, W., Xiao, J., Tian, Y., Chen, J., Singh, A., "Correlation between damage evolution and resistivity reaction of concrete in-filled with graphene nanoplatelets", ***Construction and Building Materials***, Vol. 208, (2019), 482–491. https://doi.org/10.1016/j.conbuildmat.2019.03.036
66. Xu, Y., Fan, Y., "Effect of Graphene Oxide the Concrete on Resistance to Chloride Ion Permeability", In ***IOP Conference Series: Materials Science and Engineering***, July 2018, IOP Publishing, Vol. 394, No. 3, (2018), 032020. https://doi.org/10.1088/1757-899X/394/3/032020
67. Somasri, M., Kumar, B. N., "Graphene oxide as Nano material in high strength self-compacting concrete", ***Materials Today: Proceedings***, Vol. 43, No. 2, (2021), 2280-2289. https://doi.org/10.1016/j.matpr.2020.12.1085
68. Lv, S., Ma, Y., Qiu, C., Sun, T., Liu, J., Zhou, Q., "Effect of graphene oxide nanosheets of microstructure and mechanical properties of cement composites", ***Construction and Building Materials***, Vol. 49, (2013), 121-127. https://doi.org/10.1016/j.conbuildmat.2013.08.022
69. Gong, K., Pan, Z., Korayem, A. H., Qiu, L., Li, D., Collins, F., Wang, C. M., Duan, W. H., "Reinforcing effects of graphene oxide on portland cement paste", ***Journal of Materials in Civil Engineering***, Vol. 27, No. 2, (2014), A4014010. https://doi.org/10.1061/(ASCE)MT.1943-5533.0001125
70. Chuah, S., Pan, Z., Sanjayan, J. G., Wang, C. M., Duan, W. H., "Nano reinforced cement and concrete composites and new perspective from graphene oxide", ***Construction and Building Materials***, Vol. 73, (2014), 113-124. http://doi.org/10.1016/j.conbuildmat.2014.09.040
71. Jiang, W., Li, X., Lv, Y., Zhou, M., Liu, Z., Ren, Z., Yu, Z., "Cement-Based Materials Containing Graphene Oxide and Polyvinyl Alcohol Fiber: Mechanical Properties, Durability, and Microstructure", ***Nanomaterials***, Vol. 8, No. 9, (2018), 638. https://doi.org/10.3390/nano8090638
72. Song, H. W., Lee, C. H., Ann, K. Y., "Factors influencing chloride transport in concrete structures exposed to marine environments", ***Cement and Concrete Composites***, Vol. 30, No. 2, (2008), 113-121. https://doi.org/10.1016/j.cemconcomp.2007.09.005

73. Touil, B., Ghomari, F., Bezzar, A., Khelidj, A., Bonnet, S., "Effect of temperature on chloride diffusion in saturated concrete", ***Materials Journal***, Vol. 114, No. 5, (2017), 713-721. https://hal.archives-ouvertes.fr/hal-01923475/document
74. Isteita, M., Xi, Y., "The effect of temperature variation on chloride penetration in concrete", ***Construction and Building Materials***, Vol. 156, (2017), 73-82. https://doi.org/10.1016/j.conbuildmat.2017.08.139
75. Yuan, Q., Shi, C., De Schutter, G., Audenaert, K., "Effect of temperature on transport of chloride ions in concrete, In ***Concrete Repair, Rehabilitation and Retrofitting II***; Cape Town, 24-26 November 2008, South Africa: CRC Press, (2008), 345-351. http://www.vliz.be/imisdocs/publications/265885.pdf
76. Nguyen, T. S., Lorente, S., Carcasses, M., "Effect of the environment temperature on the chloride diffusion through CEM-I and CEM-V mortars: An experimental study", ***Construction and Building Materials***, Vol. 23, No. 2, (2009), 795-803. https://doi.org/10.1016/j.conbuildmat.2008.03.004
77. Al-Khaja, W. A., "Influence of temperature, cement type and level of concrete consolidation on chloride ingress in Ordinary and high-strength concretes", ***Construction and Building Materials***, Vol. 11, No. 1, (1997), 9-13. https://doi.org/10.1016/S0950-0618(97)00004-4
78. Samson, E., Marchand, J., "Modeling the effect of temperature on ionic transport in cementitious materials", ***Cement and Concrete Research***, Vol. 37, No. 3, (2007), 455-468. https://doi.org/10.1016/j.cemconres.2006.11.008
79. Ferreira, R. M., "Optimization of RC structure performance in marine environment", ***Engineering Structures***, Vol. 32, No. 5, (2010), 1489-1494. https://doi.org/10.1016/j.engstruct.2010.02.011
80. Silva, A., Neves, R., de Brito, J., "Statistical modelling of the influential factors on chloride penetration in concrete", ***Magazine of Concrete Research***, Vol. 69, No. 5, (2017), 255-270. https://doi.org/10.1680/jmacr.16.00379
81. Jin, Z. Q., Zhao, T. J., Gao, S., Hou, B. R., "Chloride ion penetration into concrete under hydraulic pressure", ***Journal of Central South University***, Vol. 20, No. 12, (2013), 3723-3728. https://doi.org/10.1007/s11771-013-1900-5
82. Zhao, Y., Wittmann, F. H., Zhang, P., Wang, P. G., Zhao, T. J., "Penetration of Water and Chloride Dissolved in Water into Concrete under Hydraulic Pressure", ***Restoration of Buildings and Monuments***, Vol. 20, No. 2, (2014), 117–126. https://doi.org/10.1515/rbm14.20.2-0012
83. Ma, Z., Zhao, T., Zhao, Y., "Effects of hydrostatic pressure on chloride ion penetration into concrete", ***Magazine of Concrete Research***, Vol. 68, No. 17, (2016), 877-886. https://doi.org/10.1680/jmacr.15.00364
84. Lund, M. S., Sander, L. B., Grelk, B., Hansen, K. K., "Chloride Ingress into Concrete under Water Pressure", In ***Nordic Concrete Research: Proceedings of XXI Nordic Concrete Research Symposium***, Hämeenlinna, Finland, May 2011, Norway: Norsk Betongforening, No. 43, (2011), 207-210. https://nordicconcrete.net/wp-content/uploads/2011/01/Vol-43-Proceedings-Finland-2011.pdf
85. Zenunović, D., Residbegovic, N., Folic, R., "Chloride penetration through concrete cover under pressure of salty water", In ***Proceedings of the 1st International Conference on Construction Materials for Sustainable Future, CoMS_2017***, Zadar, Croatia, 19-21 April 2017, (2017), 407-413. https://www.researchgate.net/publication/316454578
86. Sharma, S., Kothiyal, N. C., "Comparative effects of pristine and ball-milled graphene oxide on physico-chemical characteristics of cement mortar nanocomposites", ***Construction and Building Materials***, Vol. 115, (2016), 256–268. https://doi.org/10.1016/j.conbuildmat.2016.04.019
87. ASTM, ***Standard Test Method for Electrical Indication of Concrete's Ability to Resist Chloride Ion Penetration***, ASTM C1202-12, ASTM International, West Conshohocken, PA, USA, (2012). https://salmanco.com/wp-content/uploads/2017/06/ASTM-c-1202.pdf
88. Lataste, J. F., Sirieix, C., Breysse, D., Frappa, M., "Electrical resistivity measurement applied to cracking assessment on reinforced concrete structures in civil engineering", ***NDT & E International***, Vol. 36, No. 6, (2003), 383-394. https://doi.org/10.1016/S0963-8695(03)00013-6
89. Azarsa, P., Gupta, R., "Electrical resistivity of concrete for durability evaluation: a review", ***Advances in Materials Science and Engineering***, Vol. 2017, (2017), 8453095. https://doi.org/10.1155/2017/8453095
90. Lu, L., Ouyang, D., "Properties of cement mortar and ultra-high strength concrete incorporating graphene oxide nanosheets", ***Nanomaterials***, Vol. 7, No. 7, (2017), 187. https://doi.org/10.3390/nano7070187
91. Siburian, R., Sihotang, H., Raja, S. L., Supeno, M., Simanjuntak, C., "New route to synthesize of graphene nano sheets", ***Oriental Journal of Chemistry***, Vol. 34, No. 1, (2018), 182. http://doi.org/10.13005/ojc/340120
92. Storm, M. M., Johnsen, R. E., Norby, P., "In situ X-ray powder diffraction studies of the synthesis of graphene oxide and formation of reduced graphene oxide", ***Journal of Solid State Chemistry***, Vol. 240, (2016), 49-54. https://doi.org/10.1016/j.jssc.2016.05.019
93. Ahmad, A., Ullah, S., Khan, A., Ahmad, W., Khan, A. U., Khan, U. A., Rahman, A. U., Yuan, Q., "Graphene oxide selenium nanorod composite as a stable electrode material for energy storage devices", ***Applied Nanoscience***, Vol. 10, No. 4, (2020), 1243-1255. https://doi.org/10.1007/s13204-019-01204-0
94. Chintalapudi, K., Pannem, R. M. R., "An intense review on the performance of Graphene Oxide and reduced Graphene Oxide in an admixed cement system", ***Construction and Building Materials***, Vol. 259, (2020), 120598. https://doi.org/10.1016/j.conbuildmat.2020.120598
95. Mahendran, R., Sridharan, D., Santhakumar, K., Selvakumar, T. A., Rajasekar, P., Jang, J. H., "Graphene oxide reinforced polycarbonate nanocomposite films with antibacterial properties", ***Indian Journal of Materials Science***, Vol. 2016, (2016), 4169409. https://doi.org/10.1155/2016/4169409
96. Eigler, S., Hirsch. A., "Chemistry with graphene and graphene oxide—challenges for synthetic chemists", ***Angewandte Chemie International Edition***, Vol. 53, No. 30, (2014), 7720-7738. https://doi.org/10.1002/anie.201402780
97. Guerrero-Contreras, J., Caballero-Briones, F., "Graphene oxide powders with different oxidation degrees, prepared by synthesis variations of the Hummers method", ***Materials Chemistry and Physics***, Vol. 153, (2015), 209-220. https://doi.org/10.1016/j.matchemphys.2015.01.005
98. Male, U., Srinivasan, P., Singu, B. S., "Incorporation of polyaniline nanofibres on graphene oxide by interfacial polymerization pathway for supercapacitor", ***International Nano Letters***, Vol. 5, No. 4, (2015), 231-240. https://doi.org/10.1007/s40089-015-0160-9
99. Hemidouche, S., Boudriche, L., Boudjemaa, A., Hamoudi, S., "Removal of lead (II) and cadmium (II) cations from water using surface-modified graphene", ***The Canadian Journal of Chemical Engineering***, Vol, 95, No. 3, (2017) 508-515. https://doi.org/10.1002/cjce.22693
100. Saleem, H., Haneef, M., Abbasi, H. Y., "Synthesis route of reduced graphene oxide via thermal reduction of chemically exfoliated graphene oxide", ***Materials Chemistry and Physics***, Vol. 204, (2018), 1-7. https://doi.org/10.1016/j.matchemphys.2017.10.020
101. Liu, L., Wang C., Wang, G., "Novel cysteic acid/reduced graphene oxide composite film modified electrode for the selective detection of trace silver ions in natural waters", ***Analytical Methods***, Vol. 5, No. 20, (2013), 5812-5822. https://doi.org/10.1039/C3AY40888D
102. Mohammed, A., Sanjayan, J. G., Duan, W. H., Nazari, A., "Incorporating graphene oxide in cement composites: A study of transport properties", ***Construction and Building Materials***, Vol. 84, (2015), 341-347. https://doi.org/10.1016/j.conbuildmat.2015.01.083

103. Wang, B., Zhao, R., "Effect of graphene nano-sheets on the chloride penetration and microstructure of the cement based composite", ***Construction and Building Materials***, Vol. 161, (2018), 715-722. https://doi.org/10.1016/j.conbuildmat.2017.12.094
104. Peng, H., Ge, Y., Cai, C. S., Zhang, Y., Liu, Z., "Mechanical properties and microstructure of graphene oxide cement-based composites", ***Construction and Building Materials***, Vol. 194, (2019), 102-109. https://doi.org/10.1016/j.conbuildmat.2018.10.234
105. Dai, J., Wang, Q., Xie, C., Xue, Y., Duan, Y. and Cui, X., "The effect of fineness on the hydration activity index of ground granulated blast furnace slag", ***Materials***, Vol. 12, No. 18, (2019), 2984. https://doi.org/10.3390/ma12182984
106. Guowen, S., Xuemao, G., Shuqiong, L., Dan, H., "Opinions on Test Method of Chloride Ions Content in "Testing Code of Concrete for Port and Waterway Engineering" [J]", ***Industrial Construction***, Vol. 35, No. 12, (2005), 8-10,7. https://en.cnki.com.cn/Article_en/CJFDTotal-GYJZ200512002.htm.
107. Wainwright, P., Rey, N., "The influence of ground granulated blastfurnace slag (GGBS) additions and time delay on the bleeding of concrete", ***Cement and Concrete Composites***, Vol. 22, No. 4, (2000), 253-257. https://doi.org/10.1016/S0958-9465(00)00024-X
108. Pan, Z., Li, T., Ruan, X., "Effect of Seasonal Characteristics of Temperature and Relative Humidity on Chloride Diffusion Process in Concrete: A Preliminary Theoretical Study", ***Sustainability***, Vol. 11, No. 22, (2019), 6330. https://doi.org/10.3390/su11226330
109. Lin, S. H., "Effective diffusion coefficient of chloride in porous concrete", ***Journal of Chemical Technology and Biotechnology***, Vol. 54, No. 2, (1992), 145-149. https://doi.org/10.1002/jctb.280540208
110. Babak, F., Abolfazl, H., Alimorad, R., Parviz, G., "Preparation and mechanical properties of graphene oxide: cement nanocomposites", ***The Scientific World Journal***, Vol. 2014, (2014), 276323. https://doi.org/10.1155/2014/276323
111. Bhojaraju, C., Mousavi, S. S., Brial, V., DiMare M., Ouellet-Plamondon, C. M., "Fresh and hardened properties of GGBS-contained cementitious composites using graphene and graphene oxide", ***Construction and Building Materials***, Vol. 300, (2021), 123902. https://doi.org/10.1016/j.conbuildmat.2021.123902
112. Song, H. W., Saraswathy, V., "Studies on the corrosion resistance of reinforced steel in concrete with ground granulated blast-furnace slag—An overview", ***Journal of Hazardous Materials***, Vol. 138, No. 2, (2006), 226–233. https://doi.org/10.1016/j.jhazmat.2006.07.022
113. Kumar, R., Bhattacharjee, B., "Porosity, pore size distribution and in situ strength of concrete", ***Cement and Concrete Research***, Vol. 33, No. 1, (2003), 155-164. https://doi.org/10.1016/S0008-8846(02)00942-0
114. Song, Y., Zhou, J. W., Bian, Z. N., Dai G. Z., "Pore structure characterization of hardened cement paste by multiple methods", ***Advances in Materials Science and Engineering***, Vol. 2019, (2019), 3726953. https://doi.org/10.1155/2019/3726953
115. Zhao, Q. L., Zhang, Y. Z., "Concentration distribution of chloride ion under the influence of the convection-diffusion coupling", ***Advances in Materials Science and Engineering***, Vol. 2017, (2017), 2076986. https://doi.org/10.1155/2017/2076986
116. Zhang, Y. Z., Li, X. Z., Wei, X. J., Yu, G. H., Li, W. G., Huang, Y. S., "Shuǐ xià suìdào hùnníngtǔ zhōng shuǐfèn yùn yí" [Water penetration in underwater concrete tunnel], ***Journal of the Chinese Ceramic Society***, Vol. 43, No. 4, (2015), 368-375. https://doi.org/10.14062/j.issn.0454-5648.2015.04.02
117. Crete, D., "chloride ingress initiation of corrosion", In ***General Guidelines for Durability Design and Redesign: DuraCrete, Probabilistic Performance Based Durability Design of Concrete Structures (contract BRPR-CT95-0132, Project BE95-1347),*** Gouda: CUR, (2000), 32–38. https://lib.ugent.be/catalog/rug01:001386862
118. Lei, M., Lin, D., Shi, C., Ma, J., Yang, W., "A structural calculation model of shield tunnel segment: Heterogeneous equivalent beam model", ***Advances in Civil Engineering***, Vol. 2018, (2018), 9637838. https://doi.org/10.1155/2018/9637838
119. Liang, M. T., Huang, R., Jhen, H. Y., "Revisited to the relationship between the free and total chloride diffusivity in concrete", ***Journal of Marine Science and Technology***, Vol. 18, No. 3, (2010), 442–448. https://doi.org/10.51400/2709-6998.1892
120. Zhu, X. H., Kang, X. J., Yang, K., Yang, C. H., "Effect of graphene oxide on the mechanical properties and the formation of layered double hydroxides (LDHs) in alkali-activated slag cement", ***Construction and Building Materials***, Vol. 132, (2017), 290-295. https://doi.org/10.1016/j.conbuildmat.2016.11.059
121. Caré, S., "Effect of temperature on porosity and on chloride diffusion in cement pastes", ***Construction and Building Materials***, Vol. 22, No. 7, (2008), 1560-1573. https://doi.org/10.1016/j.conbuildmat.2007.03.018
122. Sun, Y. M., Liang, M. T., Chang, T. P., "Time/depth dependent diffusion and chemical reaction model of chloride transportation in concrete", ***Applied Mathematical Modelling***, Vol. 36, No. 3, (2012), 1114–1122. https://doi.org/10.1016/j.apm.2011.07.053
123. Park, K. B., Lee, H. S., Wang, X. Y., "Prediction of Time-Dependent Chloride Diffusion Coefficients for Slag-Blended Concrete", ***Advances in Materials Science and Engineering***, Vol. 2017, (2017), 1901459. https://doi.org/10.1155/2017/1901459
124. Zhang, J. Z., McLaughlin, I. M., Buenfeld, N. R., "Modelling of Chloride Diffusion into Surface-treated Concrete", ***Cement and Concrete Composites***, Vol. 20, No. 4, (1998), 253-261. https://doi.org/10.1016/S0958-9465(98)00003-1
125. de Vera, G., Climent, M. A, Viqueira, E., Antón, C., Andrade, C., "A test method for measuring chloride diffusion coefficients through partially saturated concrete. Part II: The instantaneous plane source diffusion case with chloride binding consideration", ***Cement and Concrete Research***, Vol. 37, No. 5, (2007), 714–724. https://doi.org/10.1016/j.cemconres.2007.01.008
126. Saeki, T., Sasaki, K., Shinada, K., "Estimation of chloride diffusion coefficient of concrete using mineral admixtures", ***Journal of Advanced Concrete Technology***, Vol. 4, No. 3, (2006), 385-394. https://doi.org/10.3151/jact.4.385
127. Wu, L., Wang, Y., Wang, Y., Ju, X., Li, Q., "Modelling of two-dimensional chloride diffusion concentrations considering the heterogeneity of concrete materials", ***Construction and Building Materials***, Vol. 243, (2020), 118213. https://doi.org/10.1016/j.conbuildmat.2020.118213
128. Nosratzehi, N., Miri, M., "Experimental investigation on chloride diffusion coefficient of concrete containing GGBFS and GO in the Oman Sea", ***Periodica Polytechnica Civil Engineering***, Vol. 64, No. 3, (2020), 647–657. https://doi.org/10.3311/PPci.15335
129. Yao, L., Ren, L., Gong, G., Zhang, J., "Simulation of chloride diffusion in concrete based on a new mesoscopic numerical method", ***Advances in Civil Engineering***, Vol. 2020, (2020), 5318106. https://doi.org/10.1155/2020/5318106
130. Xu, J., Li, F., Zhao, J., Huang, L., "Model of time-dependent and stress-dependent chloride penetration of concrete under sustained axial pressure in the marine environment", ***Construction and Building Materials***, Vol. 170, (2018), 207–216. https://doi.org/10.1016/j.conbuildmat.2018.03.077
131. Evans, C., Richardson, M. G., "Service life of chloride-contaminated concrete structures", In ***Proceedings of the Concrete Research in Ireland Colloquium***, (2005), 131-137. http://www.ecocem.co.uk/wp-content/uploads/2016/08/ECL030_Service_Life_of_Chloride-Contaminated_Concrete.pdf
132. Yang, L., Ma, Q., Yu, B., "Analytical solution and experimental validation for dual time-dependent chloride diffusion in concrete", ***Construction and Building Materials***, Vol. 161,

(2018), 676–686. https://doi.org/10.1016/j.conbuildmat.2017.11.176
133. Jasielec, J. J., Stec, J., Szyszkiewicz-Warzecha, K., Łagosz, A., Deja, J., Lewenstam, A., Filipek, R., "Effective and apparent diffusion coefficients of chloride ions and chloride binding kinetics parameters in mortars: Non-stationary diffusion–reaction model and the inverse problem", ***Materials***, Vol. 13, No. 23, (2020), 5522. https://doi.org/10.3390/ma13235522
134. Thomas, M. D. A., Bamforth, P. B., "Modelling chloride diffusion in concrete Effect of fly ash and slag", ***Cement and Concrete Research***, Vol. 29, No. 4, (1999), 487–495. https://doi.org/10.1016/S0008-8846(98)00192-6
135. Nokken, M., Boddy, A., Hooton, R. D., Thomas, M. D. A., "Time dependent diffusion in concrete—three laboratory studies", ***Cement and Concrete Research***, Vol. 36, No. 1, (2006), 200–207. https://doi.org/10.1016/j.cemconres.2004.03.030
136. Cheng, Y. K., Karmiadji, I. W. Z., Huang, W. H., "The effect of time dependent chloride diffusion Coefficient on the Chloride Ingress in Concrete", In ***2011 International Conference on Electric Technology and Civil Engineering (ICETCE)***, Lushan, 22-24 April 2011, China: IEEE, (2011), 7098-7101. https://doi.org/10.1109/ICETCE.2011.5774709
137. Zhang, J., Zhou, X., Zhang, Y., Wang, M., Zhang, Y., "Stable process of concrete chloride diffusivity and corresponding influencing factors analysis", ***Construction and Building Materials***, Vol. 261, (2020), 119994. https://doi.org/10.1016/j.conbuildmat.2020.119994
138. Huang, D., Niu, D., Su, L., Fu., Q., "Chloride diffusion behavior of coral aggregate concrete under drying-wetting cycles", ***Construction and Building Materials***, Vol. 270, (2021), 121485. https://doi.org/10.1016/j.conbuildmat.2020.121485
139. Wang, Y., Wu, L., Wang, Y., Li, Q., Xiao, Z., "Prediction model of long-term chloride diffusion into plain concrete considering the effect of the heterogeneity of materials exposed to marine tidal zone", ***Construction and Building Materials***, Vol. 159, (2018), 297-315. https://doi.org/10.1016/j.conbuildmat.2017.10.083
140. Kim, J., Na, S., Hama, Y., "Effect of Blast-Furnace Slag Replacement Ratio and Curing Method on Pore Structure Change after Carbonation on Cement Paste", ***Materials***, Vol. 13, No. 21, (2020), 4787. https://doi.org/10.3390/ma13214787
141. Pellenq, R. J. M., Kushima, A., Shahsavari, R., Van Vlietd, K. J., Buehler, M. J., Yip, S., Ulm, F. J., "A realistic molecular model of cement hydrates", ***Proceedings of the National Academy of Sciences***, Vol. 106, No. 38, (2009), 16102–16107. https://doi.org/10.1073/pnas.0902180106
142. Stephant, S., Chomat, L., Nonat, A., Charpentier, T., "Influence of the slag content on the hydration of blended cement", In ***ICCC 2015-14th International Congress on the Chemistry of Cement***, Beijing, Oct 2015, China, (2015), Cea-02509185. https://hal-cea.archives-ouvertes.fr/cea-02509185/document